Solid Earth Discuss., 5, 2203–2281, 2013
www.solid-earth-discuss.net/5/2203/2013/
doi:10.5194/sed-5-2203-2013

Solid Earth
Discussions
Open Access

Practical analytical solutions for benchmarking of 2-D and 3-D geodynamic Stokes problems with variable viscosity

I. Yu. Popov[2], I. S. Lobanov[2], S. I. Popov[2], A. I. Popov[2], and T. V. Gerya[1]

[1]Institute of Geophysics, Department of Earth Sciences, Swiss Federal Institute of Technology Zurich (ETH), 5 Sonnegstrasse, 8092 Zurich, Switzerland
[2]St. Petersburg National Research University of Information Technologies, Mechanics and Optics, 49 Kronverkskiy, St. Petersburg, 197101, Russia

Received: 20 November 2013 – Accepted: 28 November 2013 – Published: 9 December 2013

Correspondence to: I. Yu. Popov (popov1955@gmail.com)

Published by Copernicus Publications on behalf of the European Geosciences Union.

Abstract

Geodynamic modeling often involves challenging computations involving solution of Stokes and continuity equations under condition of highly variable viscosity. Based on new analytical approach we developed generalized analytical solutions for 2-D and 3-D incompressible Stokes flows with both linearly and exponentially variable viscosity. We demonstrated how these generalized solutions can be converted into 2-D and 3-D test problems suitable for benchmarking numerical codes aimed at modeling various mantle convection and lithospheric dynamics problems. Main advantage of this new generalized approach is that large variety of benchmark solutions can be generated including relatively complex cases with open model boundaries, non-vertical gravity and variable gradients of viscosity and density fields, which are not parallel to Cartesian axes. Examples of respective 2-D and 3-D MatLab codes are provided with this paper.

1 Introduction

Numerical modeling of geodynamic processes is recognized as a challenging computational problem which requires use of advanced computational techniques and development of powerful numerical tools (e.g., Ismail-Zadeh and Tackley, 2010) and references therein). One of the major challenges concerns solving of the inertia-free Stokes equation coupled to the incompressible continuity equation in a combination with strong viscosity variations in the computational domain. Consequently, benchmarking of numerical codes against analytical and numerical solutions constrained for various mechanical and thermomechanical Stokes flow problems is a common practice in computational geodynamics (e.g., Blankenbach et al., 1989; Moresi et al., 1996; van Keken et al., 2008; Gerya and Yuen, 2003, 2007; Deubelbeiss and Kaus, 2008; Duretz et al., 2011; Gerya et al., 2013), Popov (2013). Available analytical and numerical solutions are mostly two-dimensional and include

- 2-D mantle convection with constant and variable viscosity (Hager and O'Connell, 1981; Revenaugh and Parsons, 1987; Blankenbach et al., 1989);
- 2-D thermochemical convection (van Keken et al., 1997);
- 2-D buoyancy driven flows for strongly varying viscosity (Zhong, 1996; Moresi et al., 1996; Gerya and Yuen, 2003);
- 2-D mechanical and thermomechanical channel and Couette flows for constant and variable viscosity (Turcotte and Schubert, 2002; Gerya and Yuen, 2003; Gerya, 2010);
- 2-D flow around deformable elliptic inclusions (Schmid and Podladchikov, 2003);
- 2-D Rayleigh–Taylor instability (Ramberg, 1968; Kaus and Becker, 2007);
- 2-D thermomechanical corner flows in subduction zones (van Keken et al., 2008);
- 2-D spontaneous subduction with a free surface (Schmeling et al., 2008);
- 2-D buoyancy driven flows with a free surface (Crameri et al., 2012);
- 2-D numerical sandbox experiments (Buiter et al., 2006);
- 3-D mantle convection in Cartesian geometry (Busse et al., 1993);
- 3-D mantle convection in spherical geometry (Zhong et al., 2008);
- 3-D infinitesimal and finite amplitude folding instability (Kaus and Schmalholz, 2006).

These solutions are constrained for a number of well defined model setups, which are of potential significance for various situations which numerical codes may face during real geodynamic simulations. Availability and broad range of 2-D and 3-D benchmark solutions are, therefore, critical for the development and testing of the next generation

SED
5, 2203–2281, 2013

of numerical geodynamic modeling software which aims to combine rheological complexity of constitutive laws with adaptive grid resolution to on both global and regional scales (e.g., Moresi et al., 2003; Dabrowski et al., 2008; Tackley, 2008; Stadler et al., 2010; Gerya et al., 2013).

In the present paper we aim to significantly expand availability of benchmark solutions for both 2-D and 3-D variable viscosity Stokes flows. In contrast to previous studies, we prefer not to start from any prescribed model setups but rather derive general analytical solutions, which are potentially suitable for generating a broad range of test problems. We derive generalized solutions for incompressible Stokes problems with (a) linearly and (b) exponentially variable viscosity. In the following we demonstrate how these generalized solutions can be converted into 2-D and 3-D test problems suitable for benchmarking numerical codes. Finally, based on the obtained benchmark problems, we show examples of numerical convergence tests for staggered-grid discretizations schemes (e.g., Gerya and Yuen, 2003, 2007).

2 Two-dimensional solution

2.1 Formulation of 2-D equations with variable viscosity

Consider the plane flow. 2-D Stokes equations for the case of varying viscosity has the form

$$2\eta\frac{\partial^2 v_x}{\partial x^2}+2\frac{\partial\eta}{\partial x}\frac{\partial v_x}{\partial x}+\eta\frac{\partial^2 v_x}{\partial y^2}+\eta\frac{\partial^2 v_y}{\partial y\partial x}+\frac{\partial\eta}{\partial y}\frac{\partial v_x}{\partial y}+\frac{\partial\eta}{\partial y}\frac{\partial v_y}{\partial x}-\frac{\partial P}{\partial x}=-\rho G_x, \quad (1)$$

$$\eta\frac{\partial^2 v_y}{\partial x^2}+\eta\frac{\partial^2 v_x}{\partial y\partial x}+\frac{\partial\eta}{\partial x}\frac{\partial v_x}{\partial y}+\frac{\partial\eta}{\partial x}\frac{\partial v_y}{\partial x}+2\frac{\partial\eta}{\partial y}\frac{\partial v_y}{\partial y}+2\eta\frac{\partial^2 v_y}{\partial y^2}-\frac{\partial P}{\partial y}=-\rho G_y, \quad (2)$$

$$\frac{\partial v_x}{\partial x}+\frac{\partial v_y}{\partial y}=0. \quad (3)$$

Here (v_x, v_y) is the flow velocity, $\eta = \eta(x,y)$ is the viscosity, P is the pressure, ρ is the density, (G_x, G_y) is the gravitational force. Note that Eq. (3) is the continuity equation.

Let us change the variables v_x, v_y, P in such a way that

$$\frac{\partial v_x}{\partial x} = \frac{1}{\eta}\frac{\partial u_x}{\partial x}, \quad \frac{\partial v_x}{\partial y} = \frac{1}{\eta}\frac{\partial u_x}{\partial y}, \tag{4}$$

$$\frac{\partial v_y}{\partial x} = \frac{1}{\eta}\frac{\partial u_y}{\partial x}, \quad \frac{\partial v_y}{\partial y} = \frac{1}{\eta}\frac{\partial u_y}{\partial y}. \tag{5}$$

$$\frac{1}{\eta}\frac{\partial P}{\partial x} = \frac{\partial \tilde{P}}{\partial x}, \quad \frac{1}{\eta}\frac{\partial P}{\partial y} = \frac{\partial \tilde{P}}{\partial y}. \tag{6}$$

The correctness conditions for such replacement are as follows

$$\frac{\partial}{\partial y}\left(\frac{1}{\eta}\frac{\partial u_x}{\partial x}\right) = \frac{\partial}{\partial x}\left(\frac{1}{\eta}\frac{\partial u_x}{\partial y}\right), \quad \frac{\partial}{\partial y}\left(\frac{1}{\eta}\frac{\partial u_y}{\partial x}\right) = \frac{\partial}{\partial x}\left(\frac{1}{\eta}\frac{\partial u_y}{\partial y}\right),$$

$$\frac{\partial}{\partial y}\left(\eta\frac{\partial \tilde{P}}{\partial x}\right) = \frac{\partial}{\partial x}\left(\eta\frac{\partial \tilde{P}}{\partial y}\right).$$

These conditions lead to the following correlations

$$\frac{\partial \eta}{\partial y}\frac{\partial u_x}{\partial x} = \frac{\partial \eta}{\partial x}\frac{\partial u_x}{\partial y}, \quad \frac{\partial \eta}{\partial y}\frac{\partial u_y}{\partial x} = \frac{\partial \eta}{\partial x}\frac{\partial u_y}{\partial y},$$

$$\frac{\partial \eta}{\partial y}\frac{\partial \tilde{P}}{\partial x} = \frac{\partial \eta}{\partial x}\frac{\partial \tilde{P}}{\partial y}.$$

All conditions give one the same characteristic equation:

$$\frac{\partial \eta}{\partial x}dx + \frac{\partial \eta}{\partial y}dy = 0.$$

SED
5, 2203–2281, 2013

Evidently, $\eta(x,y) = C$ is an integral of the equation. It is well known that an integral of the characteristic equation gives one good new variable. Namely, $\eta = \eta(x,y)$ is good new variable (the second coordinate should be orthogonal to the first one). Note that the assumption that the viscosity varies is now crucial because we use the viscosity as a new coordinate (instead of the spatial coordinate). Hence, the solutions of our equations, which predetermine the correctness of the replacement suggested above, are

$$u_x = \Phi(\eta), \quad u_y = \Psi(\eta), \quad \tilde{P} = \tilde{P}(\eta).$$

After the replacement, the Stokes Eqs. (1), (2) and the continuity condition (3) transform to the following form

$$2\frac{\partial^2 u_x}{\partial x^2} + \frac{\partial^2 u_x}{\partial y^2} + \frac{\partial^2 u_y}{\partial y \partial x} - \eta \frac{\partial \tilde{P}}{\partial x} = -\rho G_x, \tag{7}$$

$$\frac{\partial^2 u_y}{\partial x^2} + \frac{\partial^2 u_x}{\partial y \partial x} + 2\frac{\partial^2 u_y}{\partial y^2} - \eta \frac{\partial \tilde{P}}{\partial y} = -\rho G_y, \tag{8}$$

$$\frac{\partial u_x}{\partial x} + \frac{\partial u_y}{\partial y} = 0. \tag{9}$$

Inserting the expressions for u_x, u_y into Eqs. (7)–(9), one obtains the following equations

$$2\Phi' \frac{\partial^2 \eta}{\partial^2 x} + 2\Phi'' \left(\frac{\partial \eta}{\partial x}\right)^2 + \Phi' \frac{\partial^2 \eta}{\partial^2 y} + \Phi'' \left(\frac{\partial \eta}{\partial y}\right)^2 +$$
$$\Psi' \frac{\partial^2 \eta}{\partial y \partial x} + \Psi'' \frac{\partial \eta}{\partial y}\frac{\partial \eta}{\partial x} - \eta \tilde{P}' \frac{\partial \eta}{\partial x} = -\rho G_x, \tag{10}$$

$$2\Psi' \frac{\partial^2 \eta}{\partial^2 y} + 2\Psi'' \left(\frac{\partial \eta}{\partial y}\right)^2 + \Psi' \frac{\partial^2 \eta}{\partial^2 x} + \Psi'' \left(\frac{\partial \eta}{\partial x}\right)^2 +$$

SED
5, 2203–2281, 2013
Benchmarking of geodynamic Stokes problems with variable viscosity
I. Yu. Popov et al.

Title Page
Abstract | Introduction
Conclusions | References
Tables | Figures
◀| |▶
◀ ▶
Back | Close
Full Screen / Esc
Printer-friendly Version
Interactive Discussion

$$\Phi' \frac{\partial^2 \eta}{\partial y \partial x} + \Phi'' \frac{\partial \eta}{\partial y} \frac{\partial \eta}{\partial x} - \eta \tilde{P}' \frac{\partial \eta}{\partial y} = -\rho G_y, \tag{11}$$

$$\Phi' \frac{\partial \eta}{\partial x} + \Psi' \frac{\partial \eta}{\partial y} = 0. \tag{12}$$

2.2 Linearly varying viscosity

Our treatment is based on some assumptions. In this section we assume, first, that the viscosity η is a linear function of the Cartesian coordinates,

$$\eta = ax + by + c, \tag{13}$$

where a, b, c are non-zero constants. Second, the restriction concerning to the gravitational terms takes place: $\rho(aG_y - bG_x)$ and $\rho(bG_y + aG_x)$ are functions of one variable – viscosity. It means that ρG_y and ρG_x are functions of η only. Introduce the functions f, f_1:

$$f(\eta) = \frac{\rho(aG_y - bG_x)}{(a^2 + b^2)^2}, \quad f_1(\eta) = \frac{\rho(bG_y + aG_x)}{a^2 + b^2}. \tag{14}$$

Then one gets the following system of equations:

$$\Phi''(2a^2 + b^2) + \Psi'' ab - a\eta\tilde{P}' = -\rho G_x,$$
$$\Psi''(a^2 + 2b^2) + \Phi'' ab - a\eta\tilde{P} = -\rho G_y,$$
$$\Phi' a + \Psi' b = 0.$$

One can simply solve this algebraic system in respect to $\Phi'', \Psi'', \tilde{P}'$:

$$\Phi'' = bf(\eta), \quad \Psi'' = -af(\eta), \quad \tilde{P}' = \frac{f_1(\eta)}{\eta}. \tag{15}$$

SED
5, 2203–2281, 2013

It gives us:

$$u_x = \Phi = b\int_1^{\eta} \mathrm{d}\eta_1 \int_1^{\eta_1} \mathrm{d}\eta_2 f(\eta_2) + bc_1\eta + c_2,$$

$$u_y = \Psi = -a\int_1^{\eta} \mathrm{d}\eta_1 \int_1^{\eta_1} \mathrm{d}\eta_2 f(\eta_2) - ac_1\eta + c_3,$$

$$\tilde{P} = \int_1^{\eta} \mathrm{d}\eta_1 \frac{f_1(\eta_1)}{\eta_1} + c_4.$$

Correspondingly, one obtains v_x, v_y, P:

$$v_x = b\int_1^{\eta} \frac{\mathrm{d}\eta_1}{\eta_1} \int_1^{\eta_1} \mathrm{d}\eta_2 f(\eta_2) + bc_1 \log\eta + c_2 = b\int_1^{\eta} d\eta_2 f(\eta_2) \int_{\eta_2}^{\eta} \frac{\mathrm{d}\eta_1}{\eta_1} + bc_1 \log\eta + c_2.$$

Finally,

$$v_x = b\int_1^{\eta} d\eta_2 f(\eta_2) \log\left(\frac{\eta}{\eta_2}\right) + bc_1 \log\eta + c_2. \tag{16}$$

Analogous transformation takes place for v_y:

$$v_y = -a\int_1^{\eta} \frac{\mathrm{d}\eta_1}{\eta_1} \int_1^{\eta_1} \mathrm{d}\eta_2 f(\eta_2) - ac_1 \log\eta + c_3,$$

SED
5, 2203–2281, 2013

Benchmarking of geodynamic Stokes problems with variable viscosity

I. Yu. Popov et al.

Namely,

$$v_y = -a\int_1^{\eta} d\eta_2 f(\eta_2)\log\left(\frac{\eta}{\eta_2}\right) - ac_1\log\eta + c_3. \tag{17}$$

The expression for the pressure is as follows

$$P = \int_1^{\eta} \mathrm{d}\eta_1 f_1(\eta_1) + c_4. \tag{18}$$

Particularly, in the case of constant gravitational terms, i.e. for $f(\eta) = A = \text{const}$, $f_1(\eta) = A_1 = \text{const}$ one has:

$$v_x = bA\eta + b\tilde{c}_1\log\eta + \tilde{c}_2,$$
$$v_y = -aA\eta - a\tilde{c}_1\log\eta + \tilde{c}_3,$$
$$P = A_1\eta + \tilde{c}_4.$$

Consider more complicated case when the density is a linear function of the viscosity: $\rho = \beta_1\eta + \beta_2$. Then,

$$f(\eta) = a_1\eta + a_2, \quad f_1(\eta) = b_1\eta + b_2,$$

where constants a_1, a_2, b_1, b_2 are as follows

$$a_1 = \beta_1\frac{(aG_y - bG_x)}{(a^2+b^2)^2}, \quad a_2 = \beta_2\frac{(aG_y - bG_x)}{(a^2+b^2)^2},$$
$$b_1 = \beta_1\frac{(bG_y + aG_x)}{a^2+b^2}, \quad b_2 = \beta_2\frac{(bG_y + aG_x)}{a^2+b^2}.$$

SED
5, 2203–2281, 2013

Note that in this case the continuity equation (3) should be written in more general form:

$$\frac{\partial(\rho v_x)}{\partial x} + \frac{\partial(\rho v_y)}{\partial y} = 0. \tag{19}$$

Formulas (16)–(18) gives us

$$v_x = -b(a_1/2 + a_2 - c_1)\log\eta + \frac{1}{4}ba_1\eta^2 + ba_2\eta - \frac{1}{4}a_1b - a_2b + c_2,$$

$$v_y = a(a_1/2 + a_2 - c_1)\log\eta - \frac{1}{4}aa_1\eta^2 - aa_2\eta + \frac{1}{4}a_1a + a_2a + c_3,$$

$$P = \frac{1}{2}b_1\eta^2 + b_2\eta - \frac{1}{2}b_1 - b_2 + c_4.$$

The continuity equation (19) gives us the relation:

$$ac_2 + bc_3 = 0.$$

2.3 Exponentially varying viscosity

Let us construct the second benchmark solution. Now we assume that the viscosity is the exponential function of the Cartesian coordinates:

$$\eta = c\exp(ax + by). \tag{20}$$

General consideration up to Eqs. (10)–(12) is the same as earlier. By inserting Eq. (20) into Eqs. (10)–(12) and taking into account that

$$\frac{\partial\eta}{\partial x} = a\eta, \quad \frac{\partial\eta}{\partial y} = b\eta,$$

one obtains the following system of equations:

$$(2a^2 + b^2)(\Phi''\eta^2 + \Phi'\eta) + ab(\Psi''\eta^2 + \Psi'\eta) - a\tilde{P}'\eta^2 = -\rho G_x,$$

SED
5, 2203–2281, 2013

$$ab(\Phi''\eta^2 + \Phi'\eta) + (a^2 + 2b^2)(\Psi''\eta^2 + \Psi'\eta) - b\tilde{P}'\eta^2 = -\rho G_y,$$
$$a\Phi' + b\Psi' = 0.$$

Using the last relation, we exclude Ψ from the first two equations:

$$(a^2 + b^2)(\Phi''\eta^2 + \Phi'\eta) - a\tilde{P}'\eta^2 = -\rho G_x,$$
$$-\frac{a^3 + ab^2}{b}(\Phi''\eta^2 + \Phi'\eta) - b\tilde{P}'\eta^2 = -\rho G_y,$$
$$\Psi' = -\frac{a}{b}\Phi'. \tag{21}$$

One can see that we got linear algebraic system in respect to $(\Phi''\eta^2 + \Phi'\eta)$ and $\tilde{P}'$. The solution is as follows

$$\tilde{P}' = \frac{f_1(\eta)}{\eta^2}, \tag{22}$$
$$\Phi''\eta^2 + \Phi'\eta = bf(\eta). \tag{23}$$

Remark. It is interesting that these formulas contain the same functions $f(\eta)$, $f_1(\eta)$.

Equation (23) is well-known Euler ordinary differential equation. One can get its solution for arbitrary function f:

$$u_x = \Phi(\eta) = b\int_1^{\eta} \log\left(\frac{\eta}{\eta_1}\right)\frac{f(\eta_1)}{\eta_1}d\eta_1 + bc_1\log\eta + c_2. \tag{24}$$

Taking into account the relation (21), one obtain u_y:

$$u_y = \Psi(\eta) = -a\int_1^{\eta} \log\left(\frac{\eta}{\eta_1}\right)\frac{f(\eta_1)}{\eta_1})d\eta_1 - ac_1\log\eta + c_3. \tag{25}$$

SED
5, 2203–2281, 2013

Taking into account Eqs. (4) and (5) one obtains v_x, v_y:

$$v_x = b\int_1^{\eta}\frac{d\eta_1}{\eta_1^2}\int_1^{\eta_1}d\eta_2\frac{f(\eta_2)}{\eta_2} - bc_1\frac{1}{\eta} + bc_1 + c_2 =$$

$$b\int_1^{\eta}d\eta_2\frac{f(\eta_2)}{\eta_2}\int_{\eta_2}^{\eta}\frac{d\eta_1}{\eta_1^2} - bc_1\frac{1}{\eta} + bc_1 + c_2.$$

Hence, we get the expression for v_x and analogously, for v_y:

$$v_x = b\int_1^{\eta}d\eta_2\frac{f(\eta_2)}{\eta_2}\frac{\eta-\eta_2}{\eta\eta_2} - bc_1\frac{1}{\eta} + bc_1 + c_2, \tag{26}$$

$$v_y = -a\int_1^{\eta}d\eta_2\frac{f(\eta_2)}{\eta_2}\frac{\eta-\eta_2}{\eta\eta_2} + ac_1\frac{1}{\eta} - ac_1 + c_3. \tag{27}$$

As for the pressure, we obtain it from Eq. (22) by taking into account Eq. (6):

$$\tilde{P} = \int_1^{\eta}d\eta_1\frac{f_1(\eta_1)}{\eta_1^2} + c_4.$$

Hence,

$$P = \int_1^{\eta}d\eta_1\frac{f_1(\eta_1)}{\eta_1} + c_4. \tag{28}$$

One can compare Eqs. (26)–(28) with Eqs. (16)–(18).

For simple particular case (constant gravitational term) when $f(\eta) = A = \text{const}$, $f_1(\eta) = A_1 = \text{const}$ one has:

$$v_x = -\frac{b(A+c_1)}{\eta} - \frac{bA\log\eta}{\eta} + \tilde{c}_2,$$
$$v_y = \frac{a(A+c_1)}{\eta} + \frac{aA\log\eta}{\eta} + \tilde{c}_3,$$
$$P = A_1\log\eta + c_4 - b_1,$$

where $\tilde{c}_2 = bc_1 + c_2, \tilde{c}_3 = -ac_1 + c_3$.

For more complicated case when the density is a linear function of the viscosity $\rho = \beta_1\eta + \beta_2$, i.e.

$$f(\eta) = a_1\eta + a_2, \quad f_1(\eta) = b_1\eta + b_2,$$

where constants a_1, a_2, b_1, b_2 are the same as in the previous section. The continuity equation should be written in more general form Eq. (19). It is simple to evaluate integrals in Eqs. (26)–(28). In such a way one obtains

$$v_x = ba_1\log\eta + \frac{b(a_1-a_2-c_1)}{\eta} - ba_2\frac{\log\eta}{\eta} + \tilde{c}_2,$$
$$v_y = -aa_1\log\eta - \frac{a(a_1-a_2-c_1)}{\eta} + aa_2\frac{\log\eta}{\eta} + \tilde{c}_3,$$
$$P = b_1\eta + b_2\log\eta + \tilde{c}_4,$$

where $\tilde{c}_2 = c_2 + bc_1 + ba_2 - ba_1, \tilde{c}_3 = c_3 + aa_1 - aa_2 - ac_1, \tilde{c}_4 = c_4 - b_1$. The continuity equation (19) gives us the same relation as earlier:

$$ac_2 + bc_3 = 0.$$

SED
5, 2203–2281, 2013

3 Three-dimensional case

3.1 Formulation of 3-D equations with variable viscosity

Similar situation is in 3-D case. Particularly, we can realize the same procedure as in 2-D case with some additional limitations. The initial system of equations is as follows

$$
\begin{aligned}
&2\eta\frac{\partial^2 v_x}{\partial x^2}+2\frac{\partial\eta}{\partial x}\frac{\partial v_x}{\partial x}+\eta\frac{\partial^2 v_x}{\partial y^2}+\eta\frac{\partial^2 v_y}{\partial y\partial x}+\frac{\partial\eta}{\partial y}\frac{\partial v_x}{\partial y}+\frac{\partial\eta}{\partial y}\frac{\partial v_y}{\partial x}+\\
&\eta\frac{\partial^2 v_x}{\partial z^2}+\eta\frac{\partial^2 v_z}{\partial z\partial x}+\frac{\partial\eta}{\partial z}\frac{\partial v_x}{\partial z}+\frac{\partial\eta}{\partial z}\frac{\partial v_z}{\partial x}-\frac{\partial P}{\partial x}=-\rho G_x,\\
&\eta\frac{\partial^2 v_y}{\partial x^2}+\eta\frac{\partial^2 v_x}{\partial y\partial x}+\frac{\partial\eta}{\partial x}\frac{\partial v_x}{\partial y}+\frac{\partial\eta}{\partial x}\frac{\partial v_y}{\partial x}+2\frac{\partial\eta}{\partial y}\frac{\partial v_y}{\partial y}+2\eta\frac{\partial^2 v_y}{\partial y^2}+\\
&\eta\frac{\partial^2 v_y}{\partial z^2}+\eta\frac{\partial^2 v_z}{\partial z\partial y}+\frac{\partial\eta}{\partial z}\frac{\partial v_y}{\partial z}+\frac{\partial\eta}{\partial z}\frac{\partial v_z}{\partial y}-\frac{\partial P}{\partial y}=-\rho G_y,\\
&\eta\frac{\partial^2 v_z}{\partial x^2}+\eta\frac{\partial^2 v_x}{\partial z\partial x}+\frac{\partial\eta}{\partial x}\frac{\partial v_z}{\partial x}+\frac{\partial\eta}{\partial x}\frac{\partial v_x}{\partial z}+\eta\frac{\partial^2 v_y}{\partial z\partial y}+\frac{\partial\eta}{\partial y}\frac{\partial v_z}{\partial y}+\\
&\frac{\partial\eta}{\partial y}\frac{\partial v_y}{\partial z}+\eta\frac{\partial^2 v_z}{\partial y^2}+2\eta\frac{\partial^2 v_z}{\partial z^2}+2\frac{\partial\eta}{\partial z}\frac{\partial v_z}{\partial z}-\frac{\partial P}{\partial z}=-\rho G_z,
\end{aligned}
\tag{29}
$$

$$
\frac{\partial v_x}{\partial x}+\frac{\partial v_y}{\partial y}+\frac{\partial v_z}{\partial z}=0. \tag{30}
$$

The replacement of the variables v_x, v_y, v_z, P by $u_x, u_y, u_z, \tilde{P}$ is analogous to that in the two-dimensional case:

$$
\frac{\partial v_x}{\partial x}=\frac{1}{\eta}\frac{\partial u_x}{\partial x},\quad \frac{\partial v_x}{\partial y}=\frac{1}{\eta}\frac{\partial u_x}{\partial y}, \tag{31}
$$

SED
5, 2203–2281, 2013

Benchmarking of geodynamic Stokes problems with variable viscosity

I. Yu. Popov et al.

$$
\frac{\partial v_x}{\partial z} = \frac{1}{\eta}\frac{\partial u_x}{\partial z}, \quad \frac{\partial v_y}{\partial x} = \frac{1}{\eta}\frac{\partial u_y}{\partial x},
$$
$$
\frac{\partial v_y}{\partial y} = \frac{1}{\eta}\frac{\partial u_y}{\partial y}, \quad \frac{\partial v_y}{\partial z} = \frac{1}{\eta}\frac{\partial u_y}{\partial z},
$$
$$
\frac{\partial v_z}{\partial x} = \frac{1}{\eta}\frac{\partial u_z}{\partial x}, \quad \frac{\partial v_z}{\partial y} = \frac{1}{\eta}\frac{\partial u_z}{\partial y},
$$
$$
\frac{\partial v_z}{\partial z} = \frac{1}{\eta}\frac{\partial u_z}{\partial z}, \quad \frac{1}{\eta}\frac{\partial P}{\partial x} = \frac{\partial \tilde{P}}{\partial x},
$$
$$
\frac{1}{\eta}\frac{\partial P}{\partial y} = \frac{\partial \tilde{P}}{\partial y}, \quad \frac{1}{\eta}\frac{\partial P}{\partial z} = \frac{\partial \tilde{P}}{\partial z}.
$$

The correctness conditions for such replacement are as follows

$$
\frac{\partial \eta}{\partial y}\frac{\partial u_x}{\partial x} = \frac{\partial \eta}{\partial x}\frac{\partial u_x}{\partial y}, \quad \frac{\partial \eta}{\partial z}\frac{\partial u_x}{\partial x} = \frac{\partial \eta}{\partial x}\frac{\partial u_x}{\partial z},
$$
$$
\frac{\partial \eta}{\partial z}\frac{\partial u_x}{\partial y} = \frac{\partial \eta}{\partial y}\frac{\partial u_x}{\partial z}, \quad \frac{\partial \eta}{\partial y}\frac{\partial u_y}{\partial x} = \frac{\partial \eta}{\partial x}\frac{\partial u_y}{\partial y},
$$
$$
\frac{\partial \eta}{\partial z}\frac{\partial u_y}{\partial x} = \frac{\partial \eta}{\partial x}\frac{\partial u_y}{\partial z}, \quad \frac{\partial \eta}{\partial z}\frac{\partial u_y}{\partial y} = \frac{\partial \eta}{\partial y}\frac{\partial u_y}{\partial z},
$$
$$
\frac{\partial \eta}{\partial y}\frac{\partial u_z}{\partial x} = \frac{\partial \eta}{\partial x}\frac{\partial u_z}{\partial y}, \quad \frac{\partial \eta}{\partial z}\frac{\partial u_z}{\partial x} = \frac{\partial \eta}{\partial x}\frac{\partial u_z}{\partial z},
$$
$$
\frac{\partial \eta}{\partial z}\frac{\partial u_z}{\partial y} = \frac{\partial \eta}{\partial y}\frac{\partial u_z}{\partial z}, \quad \frac{\partial \eta}{\partial y}\frac{\partial \tilde{P}}{\partial x} = \frac{\partial \eta}{\partial x}\frac{\partial \tilde{P}}{\partial y},
$$
$$
\frac{\partial \eta}{\partial y}\frac{\partial \tilde{P}}{\partial x} = \frac{\partial \eta}{\partial x}\frac{\partial \tilde{P}}{\partial y}, \quad \frac{\partial \eta}{\partial z}\frac{\partial \tilde{P}}{\partial x} = \frac{\partial \eta}{\partial x}\frac{\partial \tilde{P}}{\partial z}.
$$

SED
5, 2203–2281, 2013

The characteristic equations for each triplet of equations, i.e. for $u_x, u_y, u_z, \tilde{P}$ are the same (analogously to 2-D case). The solutions for these conditional equations are

$$u_x = \Phi(\eta), \quad u_y = \Psi(\eta), \quad u_z = \Gamma(\eta), \quad \tilde{P} = \tilde{P}(\eta). \tag{32}$$

These relations give us correctness of the above introduced replacement for arbitrary varying viscosity (ensuring non-vanishing Jacobian). But it allows one to obtain the solution of the Stokes equations only under some assumptions about the viscosity

3.2 Linearly varying viscosity – 3-D case

Below we will assume (analogously to 2-D case, Eq. 13) that

$$\eta = ax + by + cz + e, \tag{33}$$

where a, b, c, e are non-zero constants. Moreover, we need in 3-D case the following restriction for the gravitational terms (compare with Eq. 14): $\rho G_x, \rho G_y, \rho G_z$ are functions of one variable – viscosity (for example, constants).

Making the substitution (Eq. 31) in the system (Eq. 29), one transforms it to the form

$$2\frac{\partial^2 u_x}{\partial x^2} + \frac{\partial^2 u_x}{\partial y^2} + \frac{\partial^2 u_y}{\partial y \partial x} + \frac{\partial^2 u_x}{\partial z^2} + \frac{\partial^2 u_z}{\partial z \partial x} - \eta\frac{\partial \tilde{P}}{\partial x} = -\rho G_x$$

$$\frac{\partial^2 u_y}{\partial x^2} + \frac{\partial^2 u_x}{\partial y \partial x} + 2\frac{\partial^2 u_y}{\partial y^2} + \frac{\partial^2 u_y}{\partial z^2} + \frac{\partial^2 u_z}{\partial z \partial y} - \eta\frac{\partial \tilde{P}}{\partial y} = -\rho G_y,$$

$$\frac{\partial^2 u_z}{\partial x^2} + \frac{\partial^2 u_x}{\partial z \partial x} + \frac{\partial^2 u_y}{\partial z \partial y} + \frac{\partial^2 u_z}{\partial y^2} + 2\frac{\partial^2 u_z}{\partial z^2} - \eta\frac{\partial \tilde{P}}{\partial z} = -\rho G_z, \tag{34}$$

$$\frac{\partial u_x}{\partial x} + \frac{\partial u_y}{\partial y} + \frac{\partial u_z}{\partial z} = 0. \tag{35}$$

SED
5, 2203–2281, 2013

Benchmarking of geodynamic Stokes problems with variable viscosity

I. Yu. Popov et al.

Substitution of Eq. (32) into Eq. (34), Eq. (35) leads to the following system for $\Phi, \Psi, \Gamma, \tilde{P}$:

$$\Phi''(2a^2 + b^2 + c^2) + \Psi'' ab + \Gamma'' ac - \eta a \tilde{P}' = -\rho G_x, \tag{36}$$

$$\Psi''(a^2 + 2b^2 + c^2) + \Phi'' ab + \Gamma'' bc - \eta b \tilde{P}' = -\rho G_y, \tag{37}$$

$$\Gamma''(a^2 + b^2 + 2c^2) + \Phi'' ac + \Psi'' bc - \eta c \tilde{P}' = -\rho G_z, \tag{38}$$

$$\Phi' a + \Psi' b + \Gamma' c = 0. \tag{39}$$

Hence,

$$\Phi''(a^2 + b^2 + c^2) - \eta a \tilde{P}' = -\rho G_x,$$

$$\Psi''(a^2 + b^2 + c^2) - \eta b \tilde{P}' = -\rho G_y,$$

$$-\frac{1}{c}\Phi''(ac^2 + ab^2 + a^3) - \frac{1}{c}\Psi''(bc^2 + a^2 b + b^3) - \eta c \tilde{P}' = -\rho G_z,$$

$$\Gamma' = -\frac{a}{c}\Phi' - \frac{b}{c}\Psi'.$$

The first three equations gives one an algebraic system in respect to $\Phi'', \Psi'', \tilde{P}'$. Then one get Γ'' from the initial system. To be the correct solution the obtained expressions should be functions of one variable – viscosity. It is ensured by our assumption concerning to the gravitational terms. The result is as follows:

$$\Phi'' = \frac{\rho(G_y ab + G_z ac - G_x(b^2 + c^2))}{(a^2 + b^2 + c^2)^2} = f_x(\eta), \tag{40}$$

$$\Psi'' = \frac{\rho(G_x ab + G_z bc - G_y(a^2 + c^2))}{(a^2 + b^2 + c^2)^2} = f_y(\eta), \tag{41}$$

$$\Gamma'' = \frac{\rho(G_x ac + G_y bc - G_z(a^2 + b^2))}{(a^2 + b^2 + c^2)^2} = f_z(\eta), \tag{42}$$

SED
5, 2203–2281, 2013

$$\tilde{P}' = \frac{\rho(G_x a + G_y b + G_x c)}{\eta(a^2 + b^2 + c^2)} = \frac{f_P(\eta)}{\eta}. \tag{43}$$

Here we defined four functions: $f_x(\eta), f_y(\eta), f_z(\eta), f_P(\eta)$. The obtained expressions are analogous to that in Eq. (15). Correspondingly, the integration is analogous, and one obtains

$$v_x = \int_1^\eta d\eta_2 f_x(\eta_2) \log\left(\frac{\eta}{\eta_2}\right) + c_{1x}\log\eta + c_{2x}, \tag{44}$$

$$v_y = \int_1^\eta d\eta_2 f_y(\eta_2) \log\left(\frac{\eta}{\eta_2}\right) + c_{1y}\log\eta + c_{2y}, \tag{45}$$

$$v_z = \int_1^\eta d\eta_2 f_z(\eta_2) \log\left(\frac{\eta}{\eta_2}\right) + c_{1z}\log\eta + c_{2z}, \tag{46}$$

$$P = \int_1^\eta \mathrm{d}\eta_1 f_P(\eta_1) + c_p. \tag{47}$$

Particularly, in the case of constant gravitational terms, i.e. for $f_x(\eta) = A_x = \text{const}$, $f_y(\eta) = A_y = \text{const}$, $f_z(\eta) = A_z = \text{const}$, $f_P(\eta) = A_P = \text{const}$ one has the result analogous to the 2-D case:

$$\begin{aligned}
v_x &= A_x\eta + \tilde{c}_{1x}\log\eta + \tilde{c}_{2x},\\
v_y &= A_y\eta + \tilde{c}_{1y}\log\eta + \tilde{c}_{2y},\\
v_z &= A_z\eta + \tilde{c}_{1z}\log\eta + \tilde{c}_{2z},\\
P &= A_P\eta + \tilde{c}_P.
\end{aligned}$$

SED
5, 2203–2281, 2013

Title Page
Abstract | Introduction
Conclusions | References
Tables | Figures
◀I | ▶I
◀ | ▶
Back | Close
Full Screen / Esc
Printer-friendly Version
Interactive Discussion

The continuity condition gives one the following correlation between the coefficients:

$$a\tilde{c}_{1x} + b\tilde{c}_{1y} + c\tilde{c}_{1z} = 0, \tag{48}$$

The condition

$$aA_x + bA_y + cA_z = 0$$

is valid identically (see the expression for f_x, f_y, f_z).

Consider more complicated case when the density is a linear function of the viscosity: $\rho = \beta_1\eta + \beta_2$. Then,

$$f_x(\eta) = a_1\eta + a_2, \quad f_y(\eta) = b_1\eta + b_2,$$
$$f_z(\eta) = d_1\eta + d_2, \quad f_P(\eta) = p_1\eta + p_2,$$

where constants $a_1, a_2, b_1, b_2, d_1, d_2, p_1, p_2$ are as follows

$$a_1 = \beta_1 \frac{(G_y ab + G_z ac - G_x(b^2 + c^2))}{(a^2 + b^2 + c^2)^2},$$
$$a_2 = \beta_2 \frac{(G_y ab + G_z ac - G_x(b^2 + c^2))}{(a^2 + b^2 + c^2)^2},$$
$$b_1 = \beta_1 \frac{(G_x ab + G_z bc - G_y(a^2 + c^2))}{(a^2 + b^2 + c^2)^2},$$
$$b_2 = \beta_2 \frac{(G_x ab + G_z bc - G_y(a^2 + c^2))}{(a^2 + b^2 + c^2)^2},$$
$$d_1 = \beta_1 \frac{(G_x ac + G_y bc - G_z(a^2 + b^2))}{(a^2 + b^2 + c^2)^2},$$

SED
5, 2203–2281, 2013

Benchmarking of geodynamic Stokes problems with variable viscosity

I. Yu. Popov et al.

$$d_2 = \beta_2 \frac{(G_x ac + G_y bc - G_z(a^2+b^2))}{(a^2+b^2+c^2)^2},$$

$$p_1 = \beta_1 \frac{(G_x a + G_y b + G_x c)}{(a^2+b^2+c^2)},$$

$$p_2 = \beta_2 \frac{(G_x a + G_y b + G_x c)}{(a^2+b^2+c^2)}.$$

The continuity equation (30) in this situation has more general form:

$$\frac{\partial(\rho v_x)}{\partial x} + \frac{\partial(\rho v_y)}{\partial y} + \frac{\partial(\rho v_z)}{\partial z} = 0. \tag{49}$$

In this case formulas for the velocity and the pressure preserve its form Eqs. (44)–(47) and give us

$$v_x = -(a_1/2 + a_2 - c_{1x})\log\eta + \frac{1}{4}a_1\eta^2 + a_2\eta - \frac{1}{4}a_1 - a_2 + c_{2x},$$

$$v_y = -(b_1/2 + b_2 - c_{1y})\log\eta + \frac{1}{4}b_1\eta^2 + b_2\eta - \frac{1}{4}b_1 - b_2 + c_{2y},$$

$$v_z = -(d_1/2 + d_2 - c_{1z})\log\eta + \frac{1}{4}d_1\eta^2 + d_2\eta - \frac{1}{4}d_1 - d_2 + c_{2z},$$

$$P = \frac{1}{2}p_1\eta^2 + p_2\eta - \frac{1}{2}p_1 - p_2 + c_p.$$

The continuity equation (49) leads to the relation

$$ac_{2x} + bc_{2y} + cc_{2z} = 0.$$

3.3 Exponentially varying viscosity – 3-D case.

Consider second benchmark solution (for exponential dependence of the viscosity on the Cartesian coordinates):

$$\eta = C\exp(ax + by + cz). \tag{50}$$

SED
5, 2203–2281, 2013

The assumption concerning gravitational terms is the same as earlier. General 3-D consideration is the same. By inserting Eq. (32) into the equations for $u_x, u_y, u_z, \tilde{P}$ and taking into account that

$$\frac{\partial \eta}{\partial x} = a\eta, \quad \frac{\partial \eta}{\partial y} = b\eta, \quad \frac{\partial \eta}{\partial z} = c\eta,$$

one obtains the following system of equations:

$$(2a^2 + b^2 + c^2)(\Phi''\eta^2 + \Phi'\eta) + ab(\Psi''\eta^2 + \Psi'\eta) + ac(\Gamma''\eta^2 + \Gamma'\eta) - a\tilde{P}'\eta^2 = -\rho G_x,$$
$$ab(\Phi''\eta^2 + \Phi'\eta) + (a^2 + 2b^2 + c^2)(\Psi''\eta^2 + \Psi'\eta) + bc(\Gamma''\eta^2 + \Gamma'\eta) - b\tilde{P}'\eta^2 = -\rho G_y,$$
$$ac(\Phi''\eta^2 + \Phi'\eta) + bc(\Psi''\eta^2 + \Psi'\eta) + (a^2 + b^2 + 2c^2)(\Gamma''\eta^2 + \Gamma'\eta) - c\tilde{P}'\eta^2 = -\rho G_z,$$
$$a\Phi' + b\Psi' + c\Gamma' = 0.$$

We can note that the first three equation give us the same algebraic system as in the case of linear viscosity (Eqs. 36–38), if one takes $(\Phi''\eta^2 + \Phi'\eta)$, $(\Psi''\eta^2 + \Psi'\eta)$, $(\Gamma''\eta^2 + \Gamma'\eta)$, $\eta\tilde{P}'$ as variables instead of $\Phi'', \Psi'', \Gamma'', \tilde{P}$ in the linear viscosity case. Hence, the solution of the system is as follows:

$$\Phi''\eta^2 + \Phi'\eta = f_x(\eta),$$
$$\Psi''\eta^2 + \Psi'\eta = f_y(\eta),$$
$$\Gamma''\eta^2 + \Gamma'\eta = f_z(\eta),$$
$$\tilde{P}'\eta = \frac{f_P(\eta)}{\eta}.$$

The definition of the functions f_x, f_y, f_z, f_p was given above, see Eqs. (40)–(43). Solving of these equations is analogous to the procedure in the corresponding 2-D case (exponential viscosity). By this way we come to the result:

$$v_x = \int\limits_1^{\eta} d\eta_2 \frac{f_x(\eta_2)}{\eta_2} \frac{\eta - \eta_2}{\eta\eta_2} + c_{1x}\frac{1}{\eta} + c_{2x}, \tag{51}$$

SED
5, 2203–2281, 2013

Benchmarking of geodynamic Stokes problems with variable viscosity

I. Yu. Popov et al.

$$v_y = \int\limits_1^{\eta} \mathrm{d}\eta_2 \frac{f_y(\eta_2)}{\eta_2} \frac{\eta - \eta_2}{\eta\eta_2} + c_{1y}\frac{1}{\eta} + c_{2y}. \tag{52}$$

$$v_z = \int\limits_1^{\eta} \mathrm{d}\eta_2 \frac{f_z(\eta_2)}{\eta_2} \frac{\eta - \eta_2}{\eta\eta_2} + c_{1z}\frac{1}{\eta} + c_{2z}. \tag{53}$$

$$P = \int\limits_1^{\eta} \mathrm{d}\eta_1 \frac{f_P(\eta_1)}{\eta_1} + c_p. \tag{54}$$

Here c_{1x}, c_{1y}, c_{1z}, $c_{2x}, c_{2y}, c_{2z}, c_p$ are some constants. The continuity equation gives one a relation between the coefficients:

$$ac_{1x} + bc_{1y} + cc_{1z} = 0.$$

One can compare Eqs. (51)–(54) with the results for the corresponding 2-D case (Eqs. 26–28).

For simple particular case (constant gravitational term) when $f_x(\eta) = A_x = \text{const}$, $f_y(\eta) = A_y = \text{const}$, $f_z(\eta) = A_z = \text{const}$, $f_P(\eta) = A_P = \text{const}$ one has:

$$v_x = -\frac{(A_x + c_{1x})}{\eta} - A_x\frac{\log\eta}{\eta} + \tilde{c}_{2x},$$

$$v_y = -\frac{(A_y + c_{1y})}{\eta} - A_y\frac{\log\eta}{\eta} + \tilde{c}_{2y},$$

$$v_z = -\frac{(A_z + c_{1z})}{\eta} - A_z\frac{\log\eta}{\eta} + \tilde{c}_{2z},$$

$$P = A_P\log\eta + c_p.$$

Discussion Paper | Discussion Paper | Discussion Paper | Discussion Paper

SED

5, 2203–2281, 2013

Benchmarking of geodynamic Stokes problems with variable viscosity

I. Yu. Popov et al.

Consider more complicated case when the density is a linear function of the viscosity: $\rho = \beta_1 \eta + \beta_2$. Then,

$$f_x(\eta) = a_1\eta + a_2, \quad f_y(\eta) = b_1\eta + b_2,$$
$$f_z(\eta) = d_1\eta + d_2, \quad f_P(\eta) = p_1\eta + p_2,$$

where constants $a_1, a_2, b_1, b_2, d_1, d_2, p_1, p_2$ have been determined in the previous section. Here we use the continuity equation in the form (49). In this case Eqs. (51)–(54) give us

$$v_x = a_1 \log\eta + \frac{(a_1 - a_2 - c_{1x})}{\eta} - a_2 \frac{\log\eta}{\eta} + \tilde{c}_{2x},$$
$$v_y = b_1 \log\eta + \frac{(b_1 - b_2 - c_{1y})}{\eta} - b_2 \frac{\log\eta}{\eta} + \tilde{c}_{2y},$$
$$v_z = d_1 \log\eta + \frac{(d_1 - d_2 - c_{1y})}{\eta} - d_2 \frac{\log\eta}{\eta} + \tilde{c}_{2y},$$
$$P = p_1\eta + p_2 \log\eta + \tilde{c}_P,$$

where $\tilde{c}_{2x} = c_{2x} + c_{1x} + a_2 - a_1$, $\tilde{c}_{2y} = c_{2y} + c_{1y} + b_2 - b_1$, $\tilde{c}_{2z} = c_{2z} + c_{1z} + d_2 - d_1$, $\tilde{c}_P = c_p - p_1$. The continuity equation (49) leads to the relation

$$a\tilde{c}_{2x} + b\tilde{c}_{2y} + c\tilde{c}_{2z} = 0.$$

4 Example problems and numerical convergence tests

The scheme of algorithm testing is conventional. We have obtained particular solutions of the Stokes and continuity equations for two types of viscosity variations. Let us choose a domain, e.g., a rectangle in 2-D case. Calculate values of velocity and pressure given by our analytical solution and take this values as the boundary conditions. Then, due to the uniqueness theorem the solution of the boundary problem in

Discussion Paper | Discussion Paper | Discussion Paper | Discussion Paper |
SED
5, 2203–2281, 2013
Benchmarking of geodynamic Stokes problems with variable viscosity
I. Yu. Popov et al.

the domain should coincide with our analytical solution. Let us compute the solution of the boundary problem by a numerical method. Comparison of the result with the exact analytical solution shows the quality of the numerical algorithm. In the present paper, we used standard 2-D and 3-D stress-conservative finite-differences on staggered regularly spaced grid for obtaning numerical solutions (Gerya et al., 2010). Respective MatLab programs for 2-D and 3-D cases are provided as suplements to this paper.

4.1 2-D example

4.1.1 Linearly varying viscosity

Consider a simple example of such flow in a rectangle $0 \le x \le x_{\mathrm{size}}, 0 \le y \le y_{\mathrm{size}}$. We assume that $\eta = ax + by + c$. We will mark the exact solution obtained in Sect. 2 as $v_{x,\mathrm{a}}, v_{y,\mathrm{a}}, P_{\mathrm{a}}$. It is the solution of the boundary problem in the rectangle Ω with the following conditions at the boundary $\partial\Omega = \{x = 0, x = x_{\mathrm{size}}, y = 0, y = y_{\mathrm{size}}\}$:

$$v_y|_{\partial\Omega} = v_{y,\mathrm{a}}, \quad v_x|_{\partial\Omega} = v_{x,\mathrm{a}}.$$

Let us compute the velocity and pressure with using of finite-difference scheme. The corresponding solution is marked as $v_{x,\mathrm{n}}, v_{y,\mathrm{n}}, P_{\mathrm{n}}$. The deviation of these values from the exact solution $(v_{x,\mathrm{n}} - v_{x,\mathrm{a}}, v_{y,\mathrm{n}} - v_{y,\mathrm{a}}, P_{\mathrm{n}} - P_{\mathrm{a}})$ is related with the error of the numerical scheme We calculate the relative errors of three types: L_∞, L_1, L_2 for different viscosity contrasts, i.e. different values of the coefficients a, b. We test the program Stokes2-D-variable-viscosity1 from Gerya (2010). The results are presented at Figs. 1–6. Namely, Figs. 1–3 correspond to low viscosity contrast, Figs. 4–6 – to high viscosity contrast. Particularly, Figs. 1 and 4 show pressure and velocity components distributions. Figures 2 and 4 characterizes the viscosity and the density distributions. Figures 3 and 6 contain plots of relative errors via the grid resolutions in logarithmic scale. The viscosity contrast, i.e. the values of the coefficients in the expression for the viscosity, is determined by given values of the viscosity at three rectangle corners. The value of the viscosity at the initial rectangle corner is 1, η_2, η_3 are the values of the viscosity at two adjacent corners. At all figures "n" means "numerical solution", "a" means "analytical solution" (benchmark).

For the case of linearly varying viscosity we made calculations for the following system parameters:

$$x_{\text{size}} = y_{\text{size}} = 1, G_x = 0, G_y = 10,$$
$$\eta_1 = 1, \beta_1 = 1, \beta_2 = 3 \times 10^3,$$
$$c = \eta_1, a = (\eta_3 - \eta_1)/x_{\text{size}}, b = (\eta_2 - \eta_1)/y_{\text{size}},$$
$$\rho = \beta_1(ax + by + c) + \beta_2.$$

One can see that there is rather high accuracy of the numerical approach. We observe the conventional situation – L_∞-error is the largest among the considered errors norms, and L_1-error and L_2-error are similar. The calculations show that one has good convergence of the numerical scheme for small viscosity contrast, but it is not so for high viscosity contrast (compare Figs. 3 and 6).

To describe in more details the dependence of the error on the viscosity contrast we fill tables with errors for different values of η_2, η_3 (see Appendix, Tables A1–A9).

4.1.2 Exponentially varying viscosity

The case of exponentially varying viscosity is treated analogously. To have a possibility of comparison with the case of linearly varying viscosity we take the same system parameters (geometrical size, gravitational terms and the dependence of the density on the viscosity) with the same viscosity contrast (i.e. the values of the viscosity at the rectangle corners)

$$C = \eta_1, \quad a = (\log(\eta_3) - \log(\eta_1))/x_{\text{size}},$$
$$b = (\log(\eta_2) - \log(\eta_1))/y_{\text{size}},$$
$$\eta = C \exp(ax + by),$$

SED
5, 2203–2281, 2013

$\rho = \beta_1 \eta + \beta_2$

$x_{\text{size}} = y_{\text{size}} = 1,$

$G_x = 10, \quad G_y = 10,$

$\eta_1 = 1, \quad \beta_1 = 1, \quad \beta_2 = 3 \times 10^3,$

We deal with two cases (low and high viscosity contrasts). Figures 7–12 present the results. Namely, Figs. 7–9 correspond to the case of low viscosity contrast, Figs. 10–12 are related with the case of high viscosity contrast. There are some similarities with the previous case. Particularly, L_∞ error norm gives us the maximum relative error value among three considered error norms. We have small errors (see the velocity and pressure distributions, Figs. 7 and 10). But peculiarities are more interesting. Namely, the numerical scheme works essentially better for the case of exponentially varying viscosity than for linearly varying viscosity. We observe good convergence both for low and for high viscosity contrasts (compare Figs. 9 and 12 and, correspondingly, Figs. 3 and 6).

Dependence of the errors on the viscosity contrast for exponentially varying viscosity is presented in the Tables A10–A18 in Appendix.

4.2 3-D example

One can note that benchmark solutions for 3-D case are essentially more rare than for the corresponding 2-D situation. It is remarkable that the suggested approach allows us to obtain such solutions for 3-D Stokes and continuity equations. As earlier, we consider the cases of linearly and exponentially varying viscosity.

4.2.1 Linearly varying viscosity

The statement of the problem is absolutely analogous to the previous case. In 3-D space we consider a parallelepiped Ω: $0 \le x \le x_{\text{size}}, 0 \le y \le y_{\text{size}}, 0 \le z \le z_{\text{size}}$. We assume that $\eta = ax + by + cz + e$. We will mark the exact solution obtained in Sect. 3

SED
5, 2203–2281, 2013

as $v_{x,\mathrm{a}}, v_{y,\mathrm{a}}, v_{z,\mathrm{a}}, P_\mathrm{a}$. Due to the uniqueness theorem, it is the solution of the boundary problem in the parallelepiped Ω with the following conditions at the boundary $\partial\Omega = \{x = 0, x = x_\mathrm{size}, y = 0, y = y_\mathrm{size}, z = 0, z = z_\mathrm{size}\}$:

$$v_x|_{\partial\Omega} = v_{x,\mathrm{a}}, v_y|_{\partial\Omega} = v_{y,\mathrm{a}}, v_z|_{\partial\Omega} = v_{z,\mathrm{a}}.$$

Let us compute the velocity and pressure with using of chosen finite-difference algorithm. The corresponding numerical solution is marked as $v_{x,\mathrm{n}}, v_{y,\mathrm{n}}, v_{z,\mathrm{n}}, P_\mathrm{n}$. The deviation of these values from the exact solution $(v_{x,\mathrm{n}} - v_{x,\mathrm{a}}, v_{y,\mathrm{n}} - v_{y,\mathrm{a}}, v_{z,\mathrm{n}} - v_{z,\mathrm{a}}, P_\mathrm{n} - P_\mathrm{a})$ is related with the error of the numerical scheme. As in 2-D case, we consider three error norms: L_∞, L_1, L_2. We deal with cases of low and high viscosity contrasts. Coefficients a, b, c, e in the viscosity formula are determined through given viscosity values $(\eta_1 = 1, \eta_2, \eta_3, \eta_4)$ at four adjacent parallelepiped vertices. We choose the following system parameters:

$$e = \eta_1, \quad a = (\eta_3 - \eta_1)/x_\mathrm{size},$$
$$b = (\eta_2 - \eta_1)/y_\mathrm{size}, \quad c = (\eta_4 - \eta_1)/z_\mathrm{size}.$$
$$\eta = ax + by + cz + e,$$
$$\rho = \beta_1\eta + \beta_2$$
$$x_\mathrm{size} = y_\mathrm{size} = z_\mathrm{size} = 1,$$
$$G_x = 10, \quad G_y = 10, \quad G_z = 0,$$
$$\eta_1 = 1, \quad \beta_1 = 1, \quad \beta_2 = 3 \times 10^3,$$

Results are presented at Figs. 13–20. Figures 13–16 correspond to the case of low viscosity contrast, Figs. 17–20 – to the case of high viscosity contrast. Figures 13, 14 and 17, 18 shows the velocity components and the pressure distribution for the central cross-section of the parallelepiped. The analytical and the numerical solutions and also the error (the solutions deviations) are shown. Figures 15 and 19 characterizes the distribution of the viscosity and the density for the same cross-section. In Figs. 16 and 20

SED
5, 2203–2281, 2013

the errors for a sequence of grid resolution used to solve the equations numerically are provided. Positive slope of the curves shows the algorithm convergence. It should be mentioned that the numerical procedure for 3-D case takes essentially greater time than in 2-D case. Qualitatively, the results are similar to that for the corresponding 2-D case. The numerical procedure works better for low viscosity contrast.

4.2.2 Exponentially varying viscosity

As in 2-D case, we consider also exponentially varying viscosity. Consideration is absolutely parallel to that in the previous section. To have a possibility of comparison we take here the same system parameters. Naturally, the viscosity and, correspondingly, density distributions are now exponential. The system parameters are chosen by the following manner:

$$C = \eta_1, \quad a = (\log(\eta_3) - \log(\eta_1))/x_{\text{size}},$$
$$b = (\log(\eta_2) - \log(\eta_1))/y_{\text{size}}, \quad c = (\log(\eta_4) - \log(\eta_1))/z_{\text{size}}.$$
$$\eta = C \exp(ax + by + cz),$$
$$\rho = \beta_1 \eta + \beta_2$$
$$x_{\text{size}} = y_{\text{size}} = z_{\text{size}} = 1,$$
$$G_x = 10, \quad G_y = 10, \quad G_z = 0,$$
$$\eta_1 = 1, \quad \beta_1 = 1, \quad \beta_2 = 3 \times 10^3,$$

The results are presented at Figs. 21–28. Figures 21–24 correspond to the case of low viscosity contrast, Figs. 25–28 – to the case of high viscosity contrast. It occurs that for exponentially varying viscosity the numerical algorithm works better than for linearly varying viscosity (compare the velocity and the pressure distributions and the corresponding errors at Figs. 21, 22, 25, and 26 with Figs. 13, 14, 17, and 18). It is in correlation with 2-D case. The algorithm convergence, i.e. the dependence of the errors

SED
5, 2203–2281, 2013

on the grid resolution is shown at Figs. 24 and 28. One can see that "exponential" case gives us better convergence than the corresponding "linear" case.

5 Conclusions

In the present paper, we developed new generalized analytical solutions for 2-D and 3-D Stokes flows with both linearly and exponentially variable viscosity. We also demonstrated how these generalized solutions can be converted into 2-D and 3-D test problems suitable for benchmarking numerical geodynamic codes. Main advantage of this new generalized approach is that large variety of benchmark problems can be easily generated including relatively complex cases with open model boundaries, non-vertical gravity and variable gradients of viscosity and density fields, which are not parallel to Cartesian axes. These solutions can be very useful for testing numerical algorithms aimed at modeling variable viscosity mantle convection and lithospheric dynamics (e.g., Ismail-Zadeh and Tackley, 2010; Gerya, 2010). Examples of respective 2-D and 3-D MatLab codes are provided with this paper.

Appendix A

Error decreasing via the grid resolution decreasing

A1 Linearly varying viscosity

Tables A1–A9 contain log rates of error decreasing via the grid resolution decreasing (the curve slope at Figs. 3 and 6 in logarithmic scale) for different viscosity contrasts in the case of linearly varying viscosity. Calculations were made for the following system parameters:

$$x_{\text{size}} = y_{\text{size}} = 1, \quad G_x = 0, \quad G_y = 10,$$

SED
5, 2203–2281, 2013

Benchmarking of geodynamic Stokes problems with variable viscosity

I. Yu. Popov et al.

$$\eta_1 = 1, \quad \beta_1 = 10^2, \quad \beta_2 = 3\times 10^3,$$
$$c = \eta_1, \quad a = (\eta_3 - \eta_1)/x_{\mathrm{size}}, \quad b = (\eta_2 - \eta_1)/y_{\mathrm{size}},$$
$$\rho = \beta_1(ax + by + c) + \beta_2.$$

Empty table cells correspond to the case when we have very small errors for all considered grid steps.

A2 Exponentially varying viscosity

Tables A10–A18 contain log rates of error decreasing with decreasing grid step (the curve slope at Figs. 9 and 12 in logarithmic scale) decreasing for different viscosity contrasts in the case of exponentially varying viscosity. System parameters are the same as in the case of linearly varying viscosity with natural changes:

$$c = \eta_1, \quad a = (\log\eta_3 - \log\eta_1)/x_{\mathrm{size}}, \quad b = (\log\eta_2 - \log\eta_1)/y_{\mathrm{size}},$$
$$\rho = \beta_1 c \exp(ax + by) + \beta_2.$$

Supplementary material related to this article is available online at http://www.solid-earth-discuss.net/5/2203/2013/sed-5-2203-2013-supplement.zip.

Acknowledgements. The work was made in the framework of Scientific and Technological Cooperation Programme Switzerland–Russia. The work was partly supported by grant 11-08-00267 of Russian Foundation for Basic Researches, grants of the President of Russia MK-2045.2013.1 and MK-1493.2013.1.

References

Albers, M.: A local mesh refinement multigrid method for 3-D convection problems with strongly variable viscosity, J. Comput. Phys., 160, 126–150, 2000.

SED
5, 2203–2281, 2013

Benchmarking of geodynamic Stokes problems with variable viscosity

I. Yu. Popov et al.

Blankenbach, B., Busse, F., Christensen, U. Cserepes, L., Gunkel, D., Hansen, U., Harder, H., Jarvis, G., Koch, M., Marquart, G., Moore, D. , Olson, P. , Schmeling H. and Schnaubelt, T.: A benchmark comparison for mantle convection codes, Geophys. J. Int., 98, 23–38, 1989.
Buiter, S. J. H., Babeyko, A. Y., Ellis, S., Gerya, T. V., Kaus, B. J. P., Kellner, A., Schreurs, G., and Yamada, Y.: The numerical sandbox: comparison of model results for a shortening and an extension experiment, in: Analogue and Numerical Modelling of Crustal-Scale Processes, Geological Society, London, Special Publications, 253, 29–64, 2006.
Busse, F. H., Christensen, U., Clever, R., Cserepes, L., Gable, C., Giannandrea, E., Guillon, L., Houseman, G., Nataf, H.-C., Ogawa, M., Parmentier, M., Sotin, C., and Travis, B.: 3-D convection at infinite Prandtl number in Cartesian geometry – a benchmark comparison, Geophys. Astro. Fluid, 75, 39–59, 1993.
Crameri, F., Schmeling, H., Golabek1, G. J., Duretz, T., Orendt, R., Buiter, S. J. H., May, D. A., Kaus, B. J. P., Gerya, T. V., and Tackley, P. J.: A comparison of numerical surface topography calculations in geodynamic modelling: an evaluation of the “sticky air” method, Geophys. J. Int., 189, 38–54, 2012.
Dabrowski, M., Krotkiewski, M., and Schmid, D. W.: MILAMIN: MATLAB-based finite-element method solver for large problems, Geochem. Geophy. Geosy., 9, Q04030, doi:10.1029/2007GC001719, 2008.
Deubelbeiss, Y. and Kaus, B. J. P.: Comparison of Eulerian and Lagrangian numerical techniques for the Stokes equations in the presence of strongly varying viscosity, Phys. Earth Planet. In., 171, 92–111, 2008.
Duretz, T., May, D. A., Gerya, T. V., and Tackley, P. J.: Discretization errors and free surface stabilization in the finite difference and marker-in-cell method for applied geodynamics: a numerical study, Geochem. Geophy. Geosy., 12, Q07004, 1–26, 2011.
Gerya, T.: Introduction to Numerical Geodynamic Modelling, Cambridge University Press, Cambridge, 2010. 2226
Gerya, T. V. and Yuen, D. A.: Characteristic-based marker-in-cell method with conservative finite-difference schemes for modeling geological flows with strongly variable transport properties, Phys. Earth Planet. In., 140, 293–318, 2003.
Gerya, T. V. and Yuen, D. A.: Robust characteristics method for modeling multiphase visco-elasto-plastic thermo-mechanical problems, Phys. Earth Planet. In., 163, 83–105, 2007.

Gerya, T. V., May, D. A., and Duretz, T.: An adaptive staggered grid finite difference method for modeling geodynamic Stokes flows with strongly variable viscosity, Geochem. Geophy. Geosy., 14, 1200–1225, doi:10.1002/ggge.20078, 2013.
Hager, B. H. and O'Connell, R. J.: A simple global model of plane dynamics and mantle convection, J. Geophys. Res., 86, 4843–4867, 1981.
Ismail-Zadeh, A. and Tackley, P.: Computational Methods in Geodynamics, Cambridge University Press, Cambridge, 2010.
Kaus, B. J. P. and Becker, T. W.: Effects of elasticity on the Rayleigh–Taylor instability: implications for large-scale geodynamics, Geophys. J. Int., 168, 843–862, 2007.
Kaus, B. J. P. and Schmalholz, S. M.: 3-D Finite amplitude folding: implications for stress evolution during crustal and lithospheric deformation, Geophys. Res. Lett., 33, L14309, 2006.
Moresi, L., Zhong, S., and Gurnis, M.: The accuracy of finite element solutions of Stokes' flow with strongly varying viscosity, Phys. Earth Planet. In., 97, 83–94, 1996.
Moresi, L., Dufour, F., and Mulhaus, H.-B.: A Lagrangian integration point finite element method for large deformation modelingof viscoelastic geomaterials, J. Comput. Phys., 184, 476–497, 2003.
Popov, A. and Sobolev, S.: SLIM3D: a tool for three-dimensional thermomechanical modeling of lithospheric deformation with elasto-visco-plastic rheology, Phys. Earth Planet. In., 171, 55–75, 2008.
Popov, I. Yu. and Makeev, I. V.: A benchmark solution for 2-D Stokes flow over cavity, Z. Angew. Math. Phys., 65, doi:10.1007/s00033-013-0364-7, accepted, 2014.
Ramberg, H.: Instability of layered system in the field of gravity. II, Phys. Earth Planet. In., 1, 448–474, 1968.
Revenaugh, J. and Parsons, B.: Dynamic topography and gravity anomalies for fluid layers whose viscosity varies exponentially with depth, Geophys. J. Int., 90, 349–368, 1987.
Schmeling, H., Babeyko, A. Y., Enns, A., Faccenna, C., Funiciello, F., Gerya, T. V., Golabek, G. J., Grigull, S., Kaus, B. J. P., Morra, G., Schmalholz, S. M., and van Hunen, J.: A benchmark comparison of spontaneous subduction models – towards a free surface, Phys. Earth Planet. In., 171, 198–223, 2008.
Schmid, D. V. and Podladchikov, Yu. Yu.: Analytical solutions for deformable elliptical inclusions in general shear, Geophys. J. Int., 155, 269–288, 2003.

Stadler, G., Gurnis, M., Burstedde, C., Wilcox, L. C., Alisic, L., and Ghattas, O.: The dynamics of plate tectonics and mantle flow: from local to global scales, Science, 329, 1033–1038, 2008.
Tackley, P. J.: Modelling compressible mantle convection with large viscosity contrasts in a three-dimensional spherical shell using the yin-yang grid, Phys. Earth Planet. In., 171, 7–18, 2008.
Tackley, P. J. and King, S. D.: Testing the tracer ratio methodfor modeling active compositional fields in mantle convection simulations, Geochem. Geophy. Geosys., 4, 8302, doi:10.1029/2001GC000214, 2003.
Torrance, K. E. and Turcotte, D. L.: Thermal convection with large viscosity variations, J. Fluid Mech., 47, 113–125, 1971.
Turcotte, D. L. and Schubert, G.: Geodynamics, Cambridge University Press, Cambridge, 2002.
van Keken, P. E., King, S. D., Schmeling, H., Christensen, U. R., Neumeister, D., and Doin, M.-P.: A comparison of methods for the modeling of thermochemical convection, J. Geophys. Res.-Sol. Ea., 102, 22477–22495, 1997.
van Keken, P. E., Currie, C., King, S. D., Behn, M. D., Cangleoncle, A., He, J., Katz, R. F., Lin, S.-C., Parmentier, E. M., Spiegelman, M., and Wang, K.: A community benchmark for subduction zone modeling, Phys. Earth Planet. In., 171, 187–197, 2008.
Zhong, S.: Analytic solutions for Stokes flow with lateral variations in viscosity, Geophys. J. Int., 124, 18–28, 1996.
Zhong, S. and Gurnis, M.: The role of plates and temperature-dependent viscosity in phase change dynamics, J. Geophys. Res., 99, 15903–15917, 1994.
Zhong, S., McNamara, A., Tan, E., Moresi, L., and Gurnis, M.: A benchmark study on mantle convection in a 3-D spherical shell using CitcomS, Geochem. Geophy. Geosy., 9, Q10017, doi:10.1029/2008GC002048, 2008.

SED
5, 2203–2281, 2013

Benchmarking of geodynamic Stokes problems with variable viscosity

I. Yu. Popov et al.

SED
5, 2203–2281, 2013

Benchmarking of geodynamic Stokes problems with variable viscosity

I. Yu. Popov et al.

Table A1. Pressure; L_∞-error.

η_3 \ η_2	2	5	20	100	300	1000	10 000
2	0.89	0.97	0.81	0.46	0.11	−0.19	−0.40
5	0.96	0.93	0.89	0.77	0.14	−0.14	−0.39
20	0.83	0.89	0.86	0.77	0.73	−0.06	−0.33
100	0.80	0.79	0.77	0.83	0.77	0.46	−0.21
300	0.76	0.76	0.77	0.79	0.83	0.79	−0.11
1000	0.49	0.61	0.73	0.77	0.77	0.83	0.14
10 000	−0.40	−0.39	−0.33	−0.21	0.13	0.41	0.80

Table A2. Pressure; L_1-error.

η_3 \ η_2	2	5	20	100	300	1000	10 000
2	1.40	0.96	1.16	0.74	0.41	0.04	−0.24
5	0.96	1.41	0.86	1.30	0.41	0.17	−0.20
20	1.16	0.86	1.37	1.21	0.60	0.24	−0.06
100	1.07	1.13	1.19	1.37	1.34	0.31	0.13
300	1.29	1.31	1.34	1.36	1.37	1.04	0.19
1000	0.37	0.51	0.77	1.16	1.33	1.36	0.20
10 000	−0.30	−0.27	−0.14	0.04	0.14	0.27	1.27

SED
5, 2203–2281, 2013

Table A3. Pressure; L_2-error.

η_3 \ η_2	2	5	20	100	300	1000	10 000
2	1.42	1.14	1.24	0.86	0.46	0.08	−0.20
5	1.13	1.44	1.03	1.30	0.57	0.23	−0.16
20	1.23	1.03	1.39	1.27	0.83	0.43	−0.01
100	1.14	1.21	1.26	1.36	1.33	0.50	0.26
300	1.27	1.27	1.29	1.33	1.34	1.17	0.40
1000	0.56	0.70	1.03	1.24	1.31	1.36	0.39
10 000	−0.21	−0.19	−0.04	0.23	0.34	0.43	1.27

SED
5, 2203–2281, 2013

Table A4. Velocity v_x; L_∞-error.

η_3 \ η_2	2	5	20	100	300	1000	10 000
2		1.67	1.41	0.77	0.34	−0.03	−0.30
5	1.63		1.23	1.04	0.36	0.06	−0.26
20	1.50	1.39		0.83	0.26	0.09	−0.17
100	0.59	0.79	0.73		1.43	0.06	−0.04
300	1.59	1.59	1.36	1.36		0.06	−0.01
1000	−0.29	−0.13	0.29	0.60	1.41		−0.01
10 000	−0.67	−0.64	−0.51	−0.21	0.07	0.03	

SED
5, 2203–2281, 2013

Table A5. Velocity v_x; L_1-error.

η_3 \ η_2	2	5	20	100	300	1000	10 000
2		2.01	1.91	1.40	0.83	0.40	0.13
5	1.51		1.96	1.93	1.09	0.60	0.16
20	1.44	1.47		2.00	1.50	0.99	0.31
100	1.17	1.43	1.56		2.09	1.39	0.70
300	1.63	1.61	1.63	1.66		1.87	1.04
1000	0.64	0.84	1.24	1.59	1.61		1.29
10 000	−0.06	−0.01	0.13	0.53	0.84	1.09	

SED
5, 2203–2281, 2013

Benchmarking of geodynamic Stokes problems with variable viscosity

I. Yu. Popov et al.

Table A6. Velocity v_x; L_2-error.

η_3 \ η_2	2	5	20	100	300	1000	10 000
2		1.99	1.81	1.20	0.70	0.29	0.01
5	1.53		1.80	1.79	0.91	0.47	0.04
20	1.47	1.54		1.81	1.09	0.77	0.20
100	1.13	1.39	1.54		2.04	0.94	0.53
300	1.64	1.63	1.63	1.61		1.49	0.77
1000	0.56	0.77	1.23	1.57	1.60		0.90
10 000	−0.19	−0.13	0.01	0.41	0.69	0.96	

SED
5, 2203–2281, 2013

Table A7. Velocity v_y; L_∞-error.

η_3 \ η_2	2	5	20	100	300	1000	10 000
2	1.75	1.63	1.47	0.64	0.03	−0.40	−0.67
5	1.67	1.44	1.37	1.23	0.24	−0.26	−0.64
20	1.40	1.23	0.97	0.83	0.34	0.09	−0.51
100	0.83	0.79	0.79	1.33	1.56	0.07	−0.21
300	1.66	1.76	1.91	1.91	1.91	0.66	0.04
1000	−0.01	0.06	0.04	0.37	0.86	1.17	0.03
10 000	−0.30	−0.27	−0.16	−0.06	−0.03	−0.03	−0.30

SED
5, 2203–2281, 2013

Table A8. Velocity v_y; L_1-error.

η_3 \ η_2	2	5	20	100	300	1000	10 000
2	1.98	1.51	1.44	1.17	0.59	0.16	−0.13
5	2.01	1.90	1.47	1.63	0.84	0.34	−0.10
20	1.90	1.94	1.94	1.57	1.30	0.73	0.06
100	1.51	1.76	2.00	2.06	1.66	0.81	0.43
300	1.87	1.96	2.04	2.09	2.07	1.44	0.76
1000	0.66	0.86	1.30	1.81	2.07	2.07	0.93
10 000	0.14	0.19	0.34	0.74	1.07	1.34	1.87

SED
5, 2203–2281, 2013

Table A9. Velocity v_y; L_2-error.

η_3 \ η_2	2	5	20	100	300	1000	10 000
2	1.99	1.53	1.49	1.14	0.51	0.07	−0.21
5	1.99	1.90	1.54	1.61	0.79	0.26	−0.19
20	1.81	1.80	1.79	1.56	1.24	0.63	−0.03
100	1.27	1.47	1.79	2.03	1.61	0.94	0.34
300	1.86	1.93	1.99	2.04	2.04	1.43	0.60
1000	0.37	0.53	0.90	1.56	1.97	2.03	0.74
10 000	0.019	0.04	0.20	0.54	0.76	0.89	1.23

SED
5, 2203–2281, 2013

Table A10. Pressure; L_∞-error.

η_3 \ η_2	2	5	20	100	300	1000	10 000
2	0.94	0.83	0.67	1.01	1.24	1.41	0.84
5	0.87	0.64	0.71	0.84	1.24	1.31	1.16
20	0.73	0.83	0.81	1.01	1.29	1.19	1.04
100	0.80	0.89	1.07	1.30	1.23	1.14	0.96
300	0.90	0.99	1.13	1.23	1.19	1.09	0.91
1000	1.04	1.13	1.14	1.11	1.09	1.03	0.86
10 000	1.19	1.13	0.70	0.91	0.87	0.84	0.71

SED
5, 2203–2281, 2013

Table A11. Pressure; L_1-error.

η_3 \ η_2	2	5	20	100	300	1000	10 000
2	1.40	0.89	1.10	1.40	1.46	1.44	1.37
5	0.89	1.13	1.17	1.34	1.41	1.43	1.36
20	0.97	1.14	1.31	1.40	1.40	1.40	1.33
100	1.20	1.36	1.31	1.39	1.39	1.36	1.26
300	1.37	1.36	1.27	1.34	1.36	1.31	1.21
1000	1.39	1.36	1.27	1.29	1.30	1.26	1.17
10 000	1.33	1.29	1.23	1.17	1.14	1.13	1.06

SED
5, 2203–2281, 2013

Table A12. Pressure; L_2-error.

η_2 / η_3	2	5	20	100	300	1000	10 000
2	1.46	1.03	1.20	1.47	1.56	1.53	1.40
5	1.03	1.13	1.23	1.39	1.53	1.51	1.39
20	1.13	1.24	1.31	1.46	1.51	1.46	1.31
100	1.27	1.39	1.39	1.46	1.43	1.37	1.23
300	1.37	1.41	1.39	1.40	1.37	1.31	1.19
1000	1.41	1.41	1.36	1.33	1.30	1.24	1.11
10 000	1.37	1.34	1.26	1.17	1.14	1.11	1.00

SED
5, 2203–2281, 2013

Table A13. Velocity v_x; L_∞-error.

η_3 \ η_2	2	5	20	100	300	1000	10 000
2		1.71	1.61	1.81	1.74	1.70	1.63
5	1.69		1.41	1.83	1.73	1.66	1.56
20	1.66	1.59	1.36	1.80	1.70	1.56	1.44
100	1.71	1.79	1.90	1.76	1.59	1.46	1.36
300	1.87	2.00	1.89	1.71	1.56	1.46	1.31
1000	1.79	1.87	1.93	1.71	1.54	1.41	1.26
10 000	1.49	1.66	1.91	1.67	1.51	1.37	1.17

SED
5, 2203–2281, 2013

Table A14. Velocity v_x; L_1-error.

η_3 \ η_2	2	5	20	100	300	1000	10 000
2		2.03	2.06	2.17	2.10	2.06	2.01
5	1.61		2.06	2.24	2.14	2.10	2.01
20	1.59	1.83	2.21	2.21	2.16	2.13	2.04
100	1.64	1.87	2.10	2.21	2.14	2.10	2.04
300	1.76	1.91	2.04	2.21	2.14	2.07	2.01
1000	1.84	1.94	2.04	2.13	2.14	2.06	1.97
10 000	1.77	1.87	1.96	2.00	2.01	2.00	1.91

SED
5, 2203–2281, 2013

Table A15. Velocity v_x; L_2-error.

η_3 \ η_2	2	5	20	100	300	1000	10 000
2		2.00	1.97	2.03	2.00	1.96	1.91
5	1.66		1.93	2.09	2.01	1.97	1.90
20	1.63	1.84	2.06	2.09	2.01	1.96	1.87
100	1.71	1.93	2.06	2.04	1.97	1.90	1.83
300	1.87	1.99	2.03	2.00	1.93	1.84	1.74
1000	1.93	2.00	2.03	2.00	1.93	1.84	1.74
10 000	1.76	1.89	1.96	1.94	1.90	1.83	1.67

SED
5, 2203–2281, 2013

Table A16. Velocity v_y; L_∞-error.

η_3 \ η_2	2	5	20	100	300	1000	10 000
2	1.76	1.67	1.83	1.87	1.71	1.71	1.56
5	1.73	1.56	1.53	2.09	1.99	1.90	1.89
20	1.67	1.46	1.37	1.96	1.89	1.86	1.84
100	1.57	1.27	1.80	1.77	1.69	1.64	1.61
300	1.27	1.80	1.79	1.67	1.57	1.53	1.50
1000	1.81	1.81	1.73	1.56	1.49	1.43	1.36
10 000	1.71	1.16	1.56	1.40	1.36	1.29	1.19

SED
5, 2203–2281, 2013

Discussion Paper | Discussion Paper | Discussion Paper | Discussion Paper |

SED
5, 2203–2281, 2013

Table A17. Velocity v_y; L_1-error.

η_3 \ η_2	2	5	20	100	300	1000	10 000
2	1.91	1.63	1.74	2.16	2.13	2.11	2.03
5	2.03	1.91	1.97	2.13	2.17	2.19	2.14
20	2.03	2.01	2.26	2.21	2.20	2.20	2.14
100	2.01	2.24	2.29	2.31	2.30	2.26	2.17
300	2.26	2.34	2.27	2.23	2.26	2.26	2.17
1000	2.24	2.24	2.23	2.17	2.17	2.17	2.16
10 000	2.07	2.10	2.11	2.11	2.09	2.07	2.07

Table A18. Velocity v_y; L_2-error.

η_3 \ η_2	2	5	20	100	300	1000	10 000
2	1.97	1.66	1.81	2.10	2.01	1.94	1.83
5	2.00	1.93	1.99	2.11	2.10	2.04	1.94
20	1.97	1.90	2.09	2.14	2.11	2.07	2.00
100	1.89	1.96	2.11	2.09	2.06	2.04	1.97
300	2.03	2.11	2.09	2.01	1.97	1.96	1.93
1000	2.11	2.06	2.04	1.96	1.91	1.87	1.86
10 000	1.96	1.94	1.93	1.87	1.83	1.77	1.71

SED
5, 2203–2281, 2013

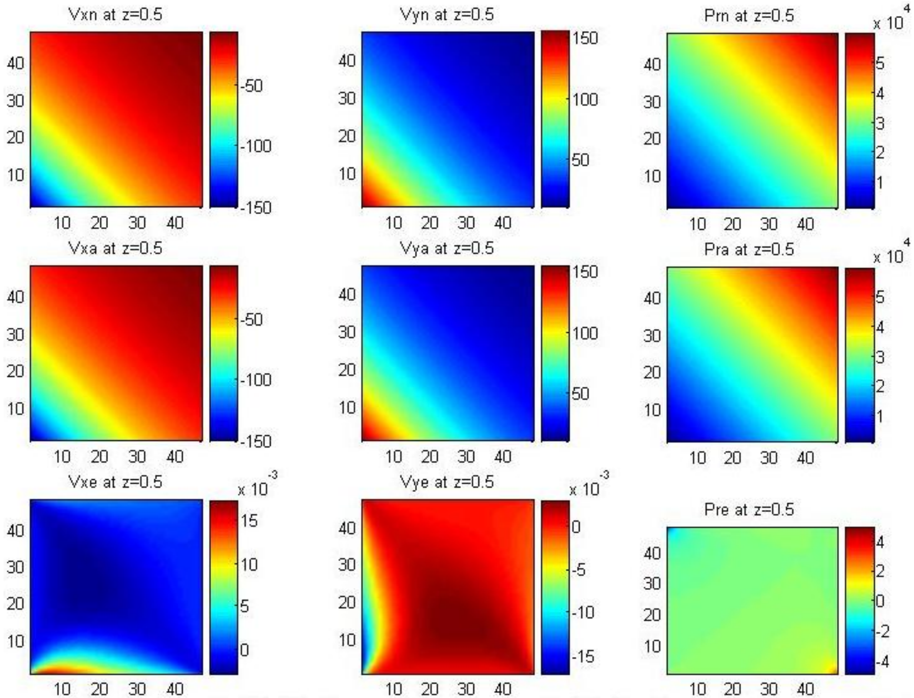

Fig. 1. Distribution of v_x, v_y and P; 2-D case, linearly varying viscosity, low viscosity contrast ($\eta_2 = \eta_3 = 5$). Here and in the following indices at the computed velocity components and pressure indicate analytical (a) and numerical (n) values and difference between them (e).

SED
5, 2203–2281, 2013

Benchmarking of geodynamic Stokes problems with variable viscosity

I. Yu. Popov et al.

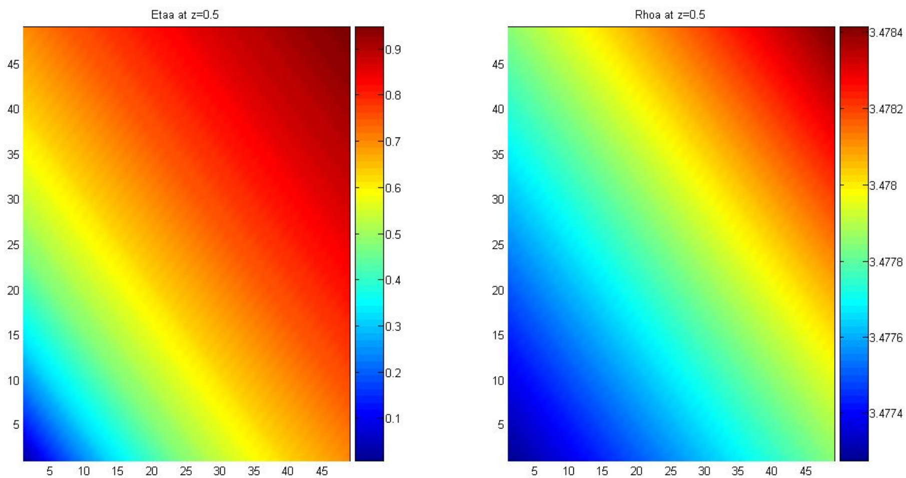

Fig. 2. Distribution of viscosity η and density ρ; 2-D case, linearly varying viscosity, low viscosity contrast ($\eta_2 = \eta_3 = 5$).

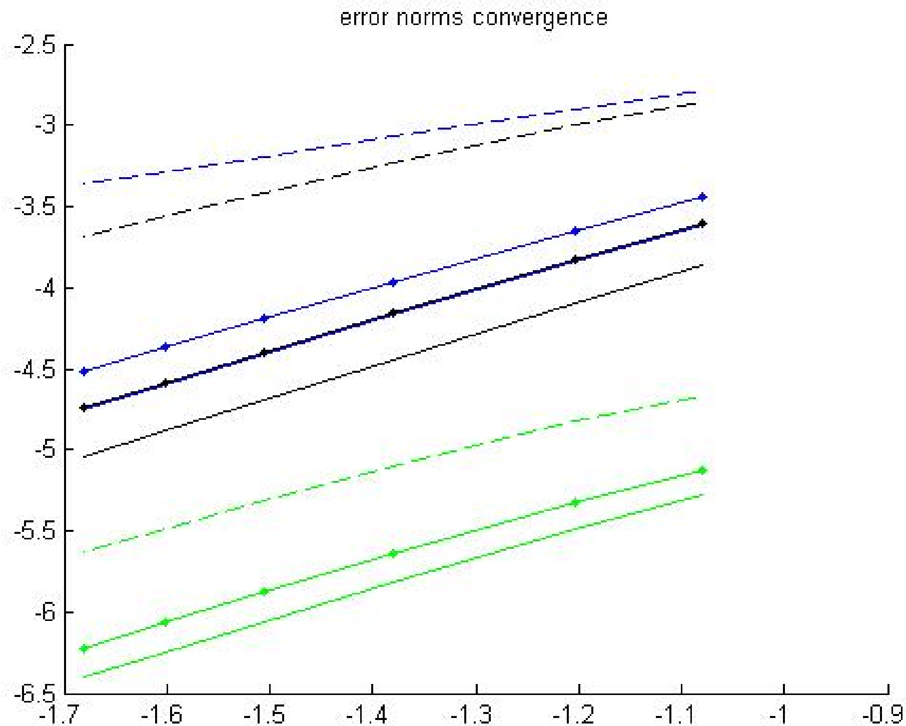

Fig. 3. Logarithm of the relative error via logarithm of the grid step; 2-D case, linearly varying viscosity, low viscosity contrast ($\eta_2 = \eta_3 = 5$); blue line – pressure, green – v_x, black – v_y; line – L_1-error, dashed line – L_∞-error, line with dots – L_2-error.

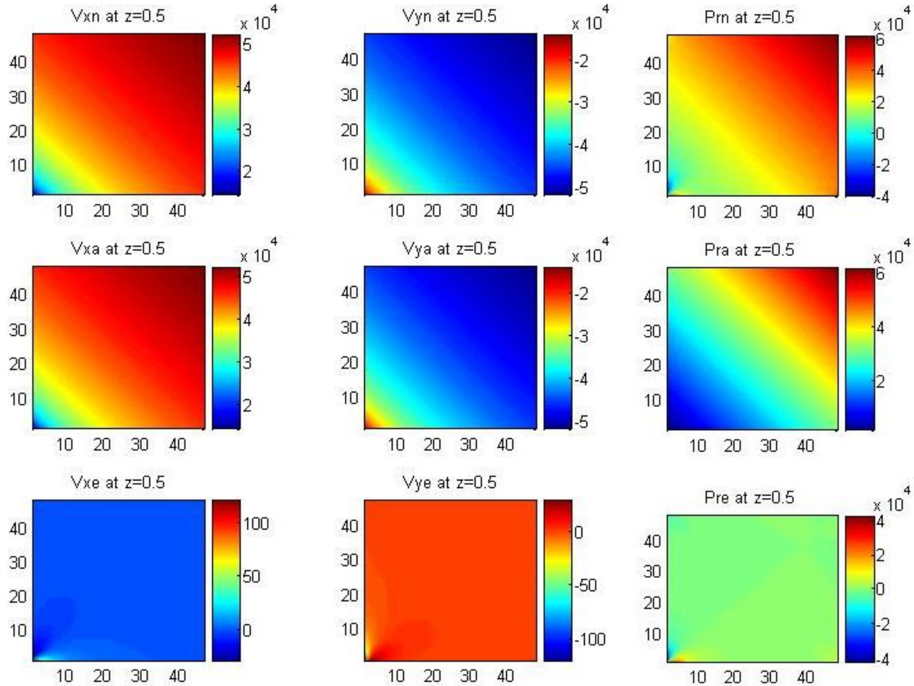

Fig. 4. Distribution of v_x, v_y and P; 2-D case, linearly varying viscosity, high viscosity contrast ($\eta_2 = \eta_3 = 100$).

SED

5, 2203–2281, 2013

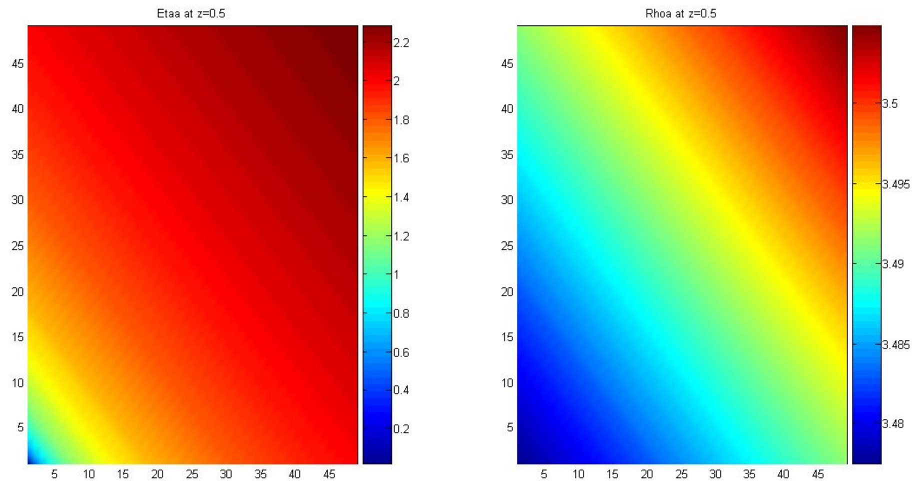

Fig. 5. Distribution of viscosity η and density ρ; 2-D case, linearly varying viscosity, high viscosity contrast ($\eta_2 = \eta_3 = 100$).

SED
5, 2203–2281, 2013

Benchmarking of geodynamic Stokes problems with variable viscosity

I. Yu. Popov et al.

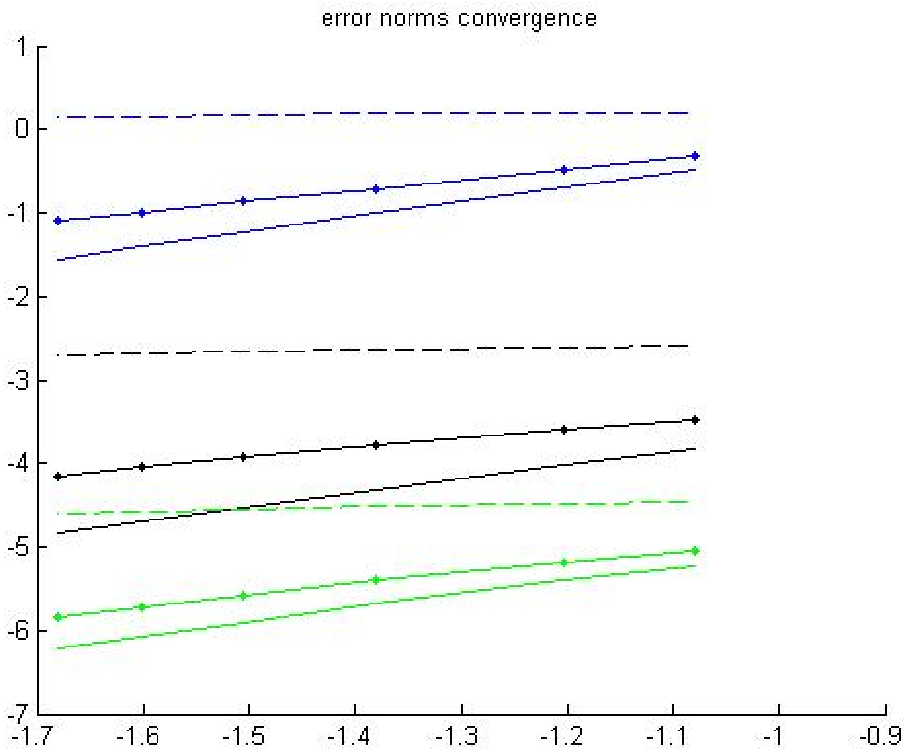

Fig. 6. Logarithm of the relative error via logarithm of the grid step; 2-D case, linearly varying viscosity, high viscosity contrast ($\eta_2 = \eta_3 = 100$); blue line – pressure, green – v_x, black – v_y; line – L_1-error, dashed line – L_∞-error, line with dots – L_2-error.

SED
5, 2203–2281, 2013

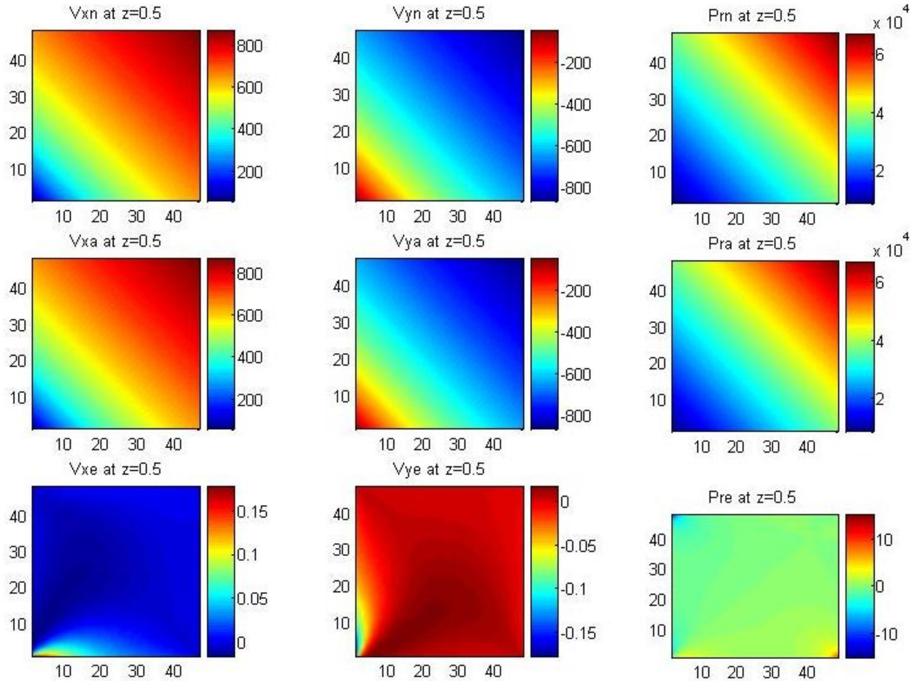

Fig. 7. Distribution of v_x, v_y and P; 2-D case, exponentially varying viscosity, low viscosity contrast ($\eta_2 = \eta_3 = 5$).

SED
5, 2203–2281, 2013

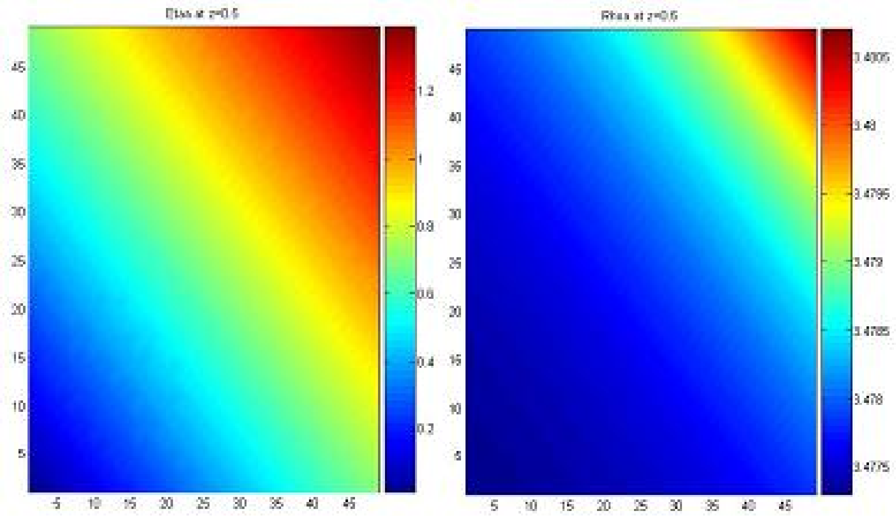

Fig. 8. Distribution of viscosity η and density ρ; 2-D case, exponentially varying viscosity, low viscosity contrast ($\eta_2 = \eta_3 = 5$).

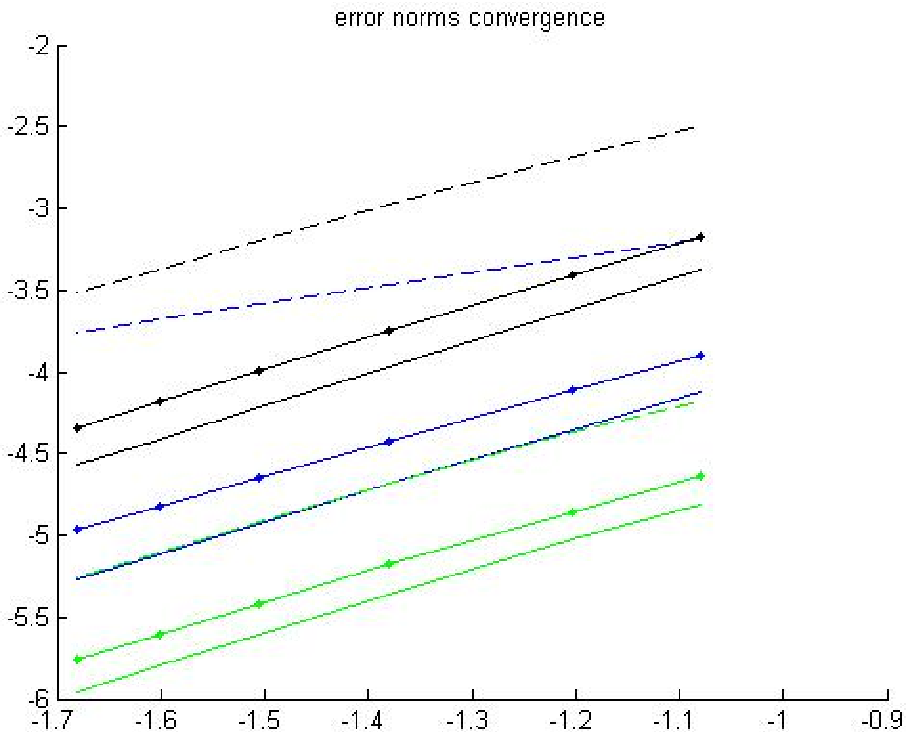

Fig. 9. Logarithm of the relative error via logarithm of the grid step; 2-D case, exponentially varying viscosity, low viscosity contrast ($\eta_2 = \eta_3 = 5$); blue line – pressure, green – v_x, black – v_y; line – L_1-error, dashed line – L_∞-error, line with dots – L_2-error.

SED
5, 2203–2281, 2013

SED

5, 2203–2281, 2013

Benchmarking of geodynamic Stokes problems with variable viscosity

I. Yu. Popov et al.

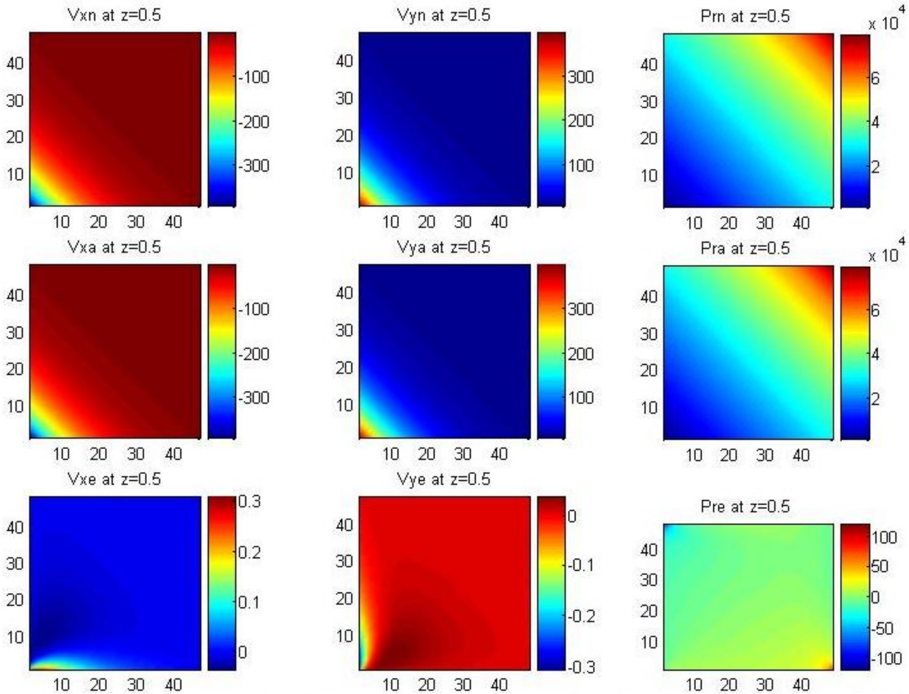

Fig. 10. Distribution of v_x, v_y and P; 2-D case, linearly varying viscosity, high viscosity contrast ($\eta_2 = \eta_3 = 100$).

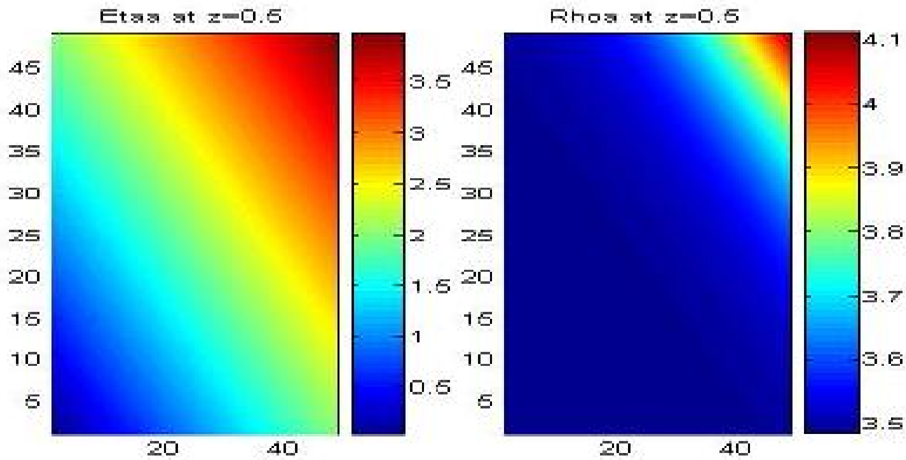

Fig. 11. Distribution of viscosity η and density ρ; 2-D case, linearly varying viscosity, high viscosity contrast ($\eta_2 = \eta_3 = 100$).

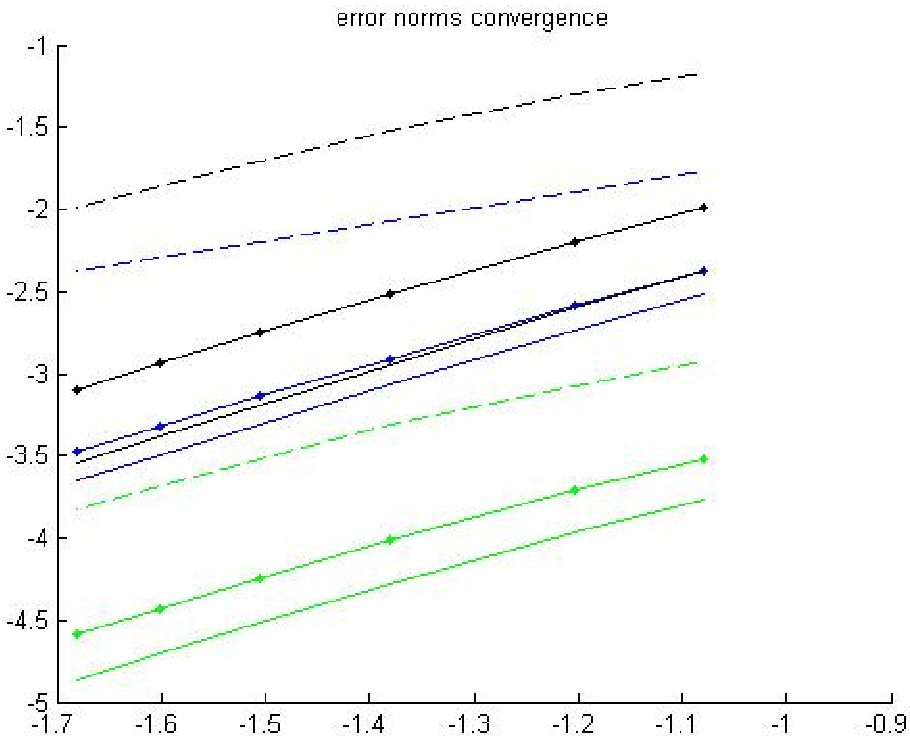

Fig. 12. Logarithm of the relative error via logarithm of the grid step; 2-D case, linearly varying viscosity, high viscosity contrast ($\eta_2 = \eta_3 = 100$); blue line – pressure, green – v_x, black – v_y; line – L_1-error, dashed line – L_∞-error, line with dots – L_2-error.

SED
5, 2203–2281, 2013

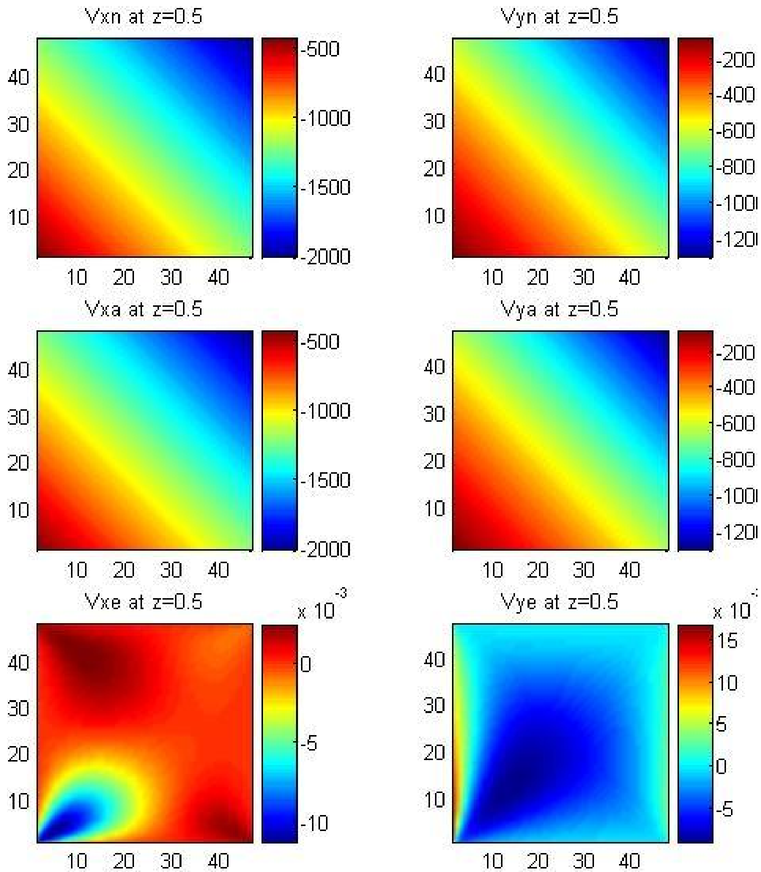

Fig. 13. Distribution of v_x and v_y; 3-D case, linearly varying viscosity, low viscosity contrast ($\eta_2 = \eta_3 = \eta_4 = 5$).

SED
5, 2203–2281, 2013

SED
5, 2203–2281, 2013

Benchmarking of geodynamic Stokes problems with variable viscosity

I. Yu. Popov et al.

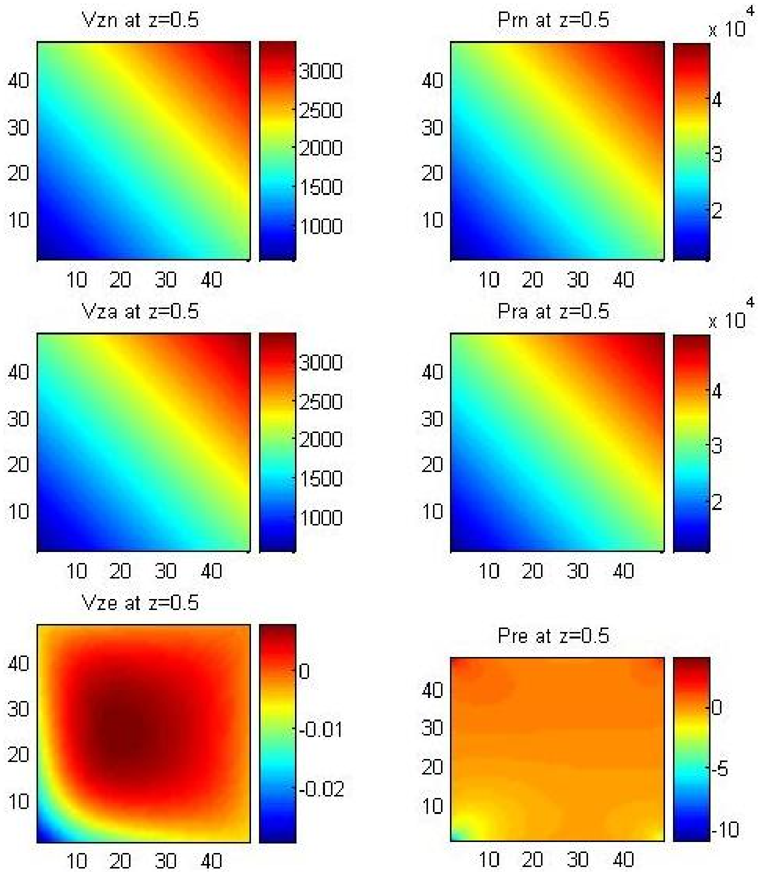

Fig. 14. Distribution of v_z and P; 3-D case, linearly varying viscosity, low viscosity contrast ($\eta_2 = \eta_3 = \eta_4 = 5$).

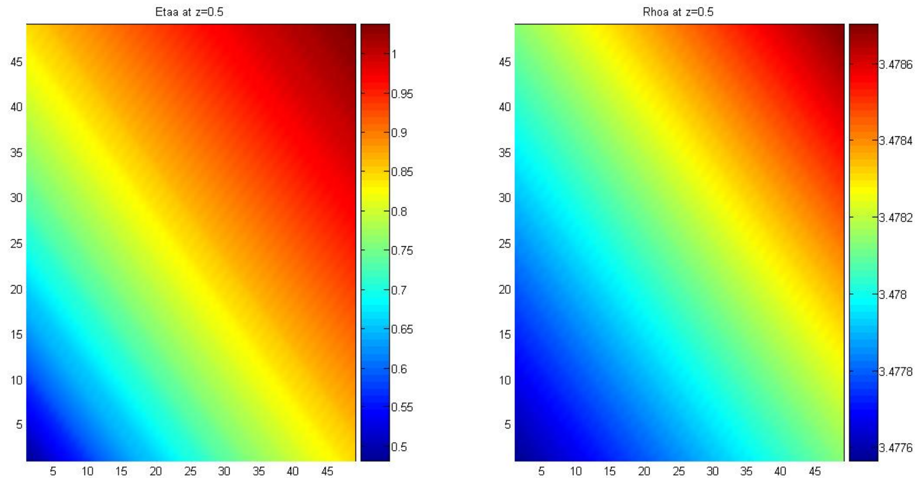

Fig. 15. Distribution of viscosity η and density ρ; 3-D case, linearly varying viscosity, low viscosity contrast ($\eta_2 = \eta_3 = \eta_4 = 5$).

SED
5, 2203–2281, 2013

Benchmarking of geodynamic Stokes problems with variable viscosity

I. Yu. Popov et al.

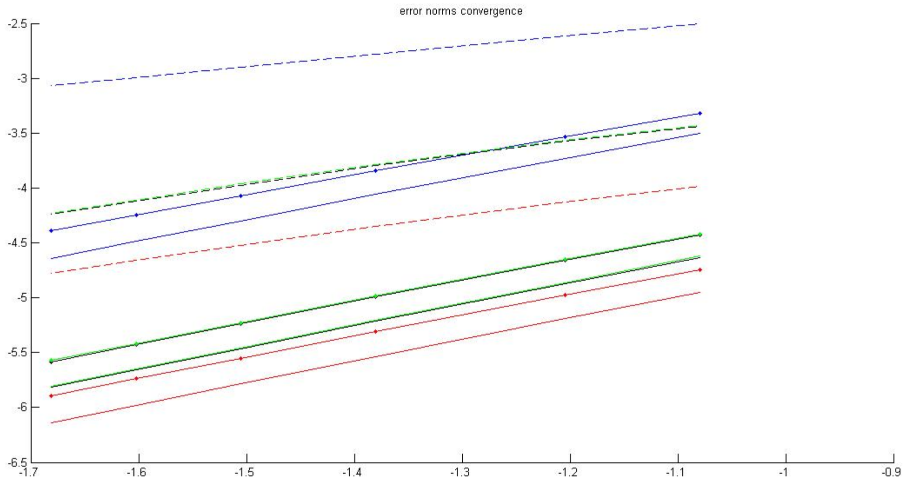

Fig. 16. Logarithm of the relative error via logarithm of the grid step; 3-D case, linearly varying viscosity, low viscosity contrast ($\eta_2 = \eta_3 = \eta_4 = 5$); blue line – pressure, red – v_x, black – v_y, green – v_z; line – L_1-error, dashed line – L_∞-error, line with dots – L_2-error.

SED
5, 2203–2281, 2013

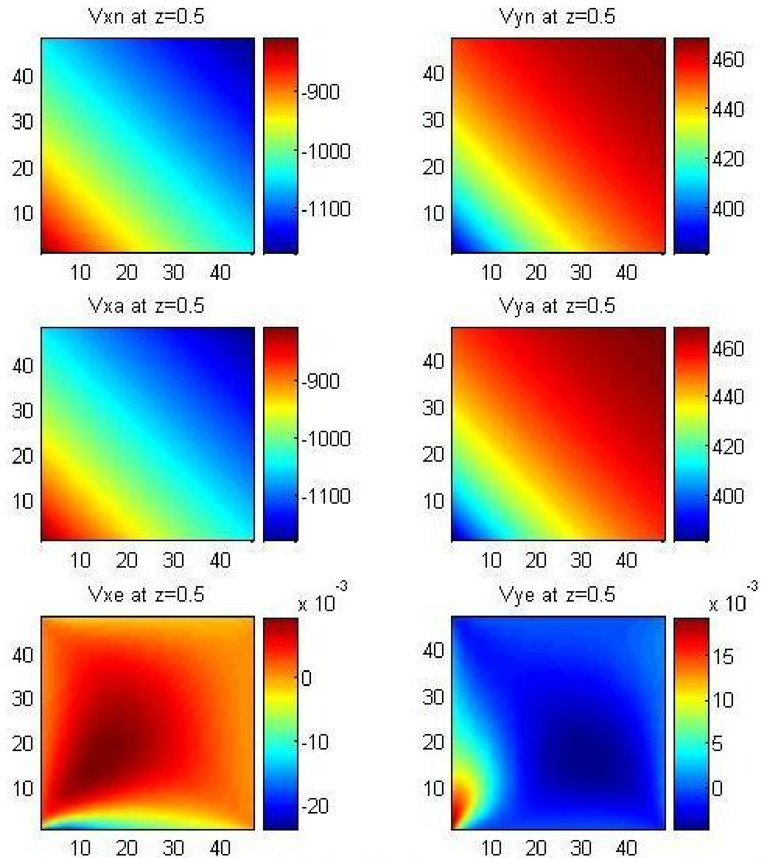

Fig. 17. Distribution of v_x and v_y; 3-D case, linearly varying viscosity, high viscosity contrast ($\eta_2 = \eta_3 = \eta_4 = 100$).

SED
5, 2203–2281, 2013

Benchmarking of geodynamic Stokes problems with variable viscosity

I. Yu. Popov et al.

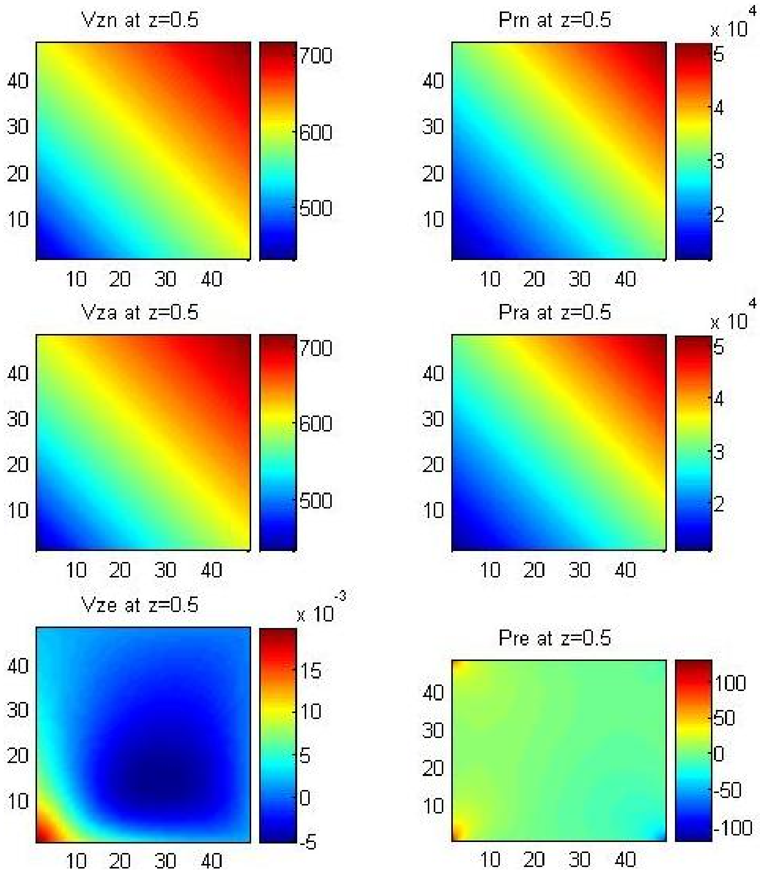

Fig. 18. Distribution of v_z and P; 3-D case, linearly varying viscosity, high viscosity contrast ($\eta_2 = \eta_3 = \eta_4 = 100$).

SED
5, 2203–2281, 2013

Benchmarking of geodynamic Stokes problems with variable viscosity

I. Yu. Popov et al.

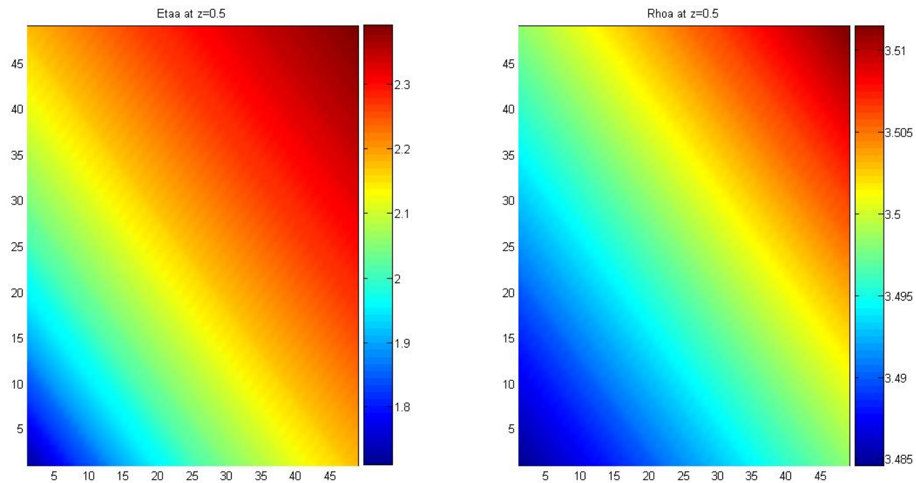

Fig. 19. Distribution of viscosity η and density ρ; 3-D case, linearly varying viscosity, high viscosity contrast ($\eta_2 = \eta_3 = \eta_4 = 100$).

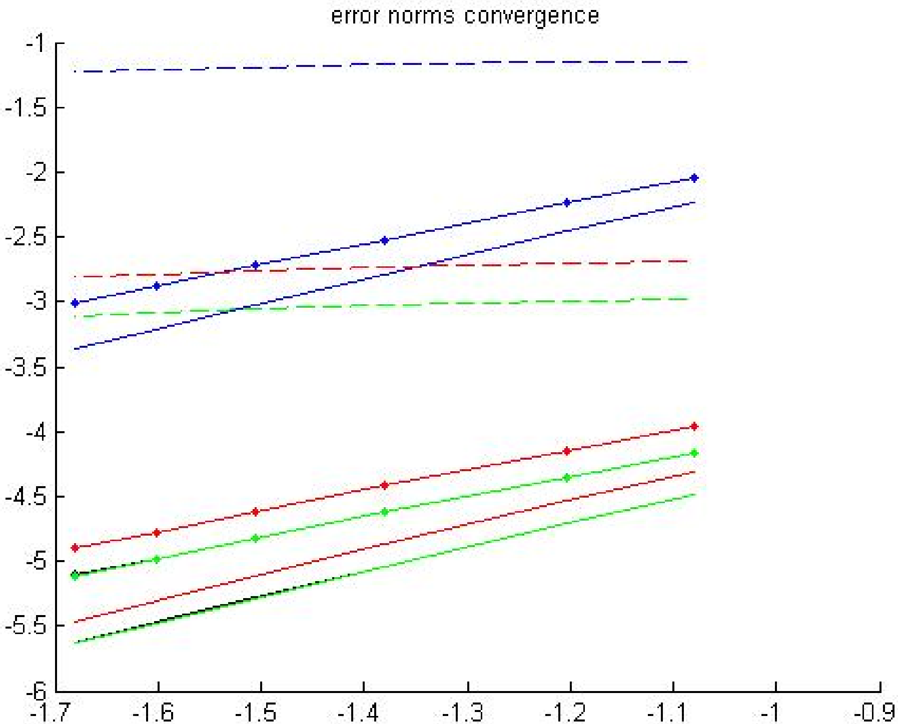

Fig. 20. Logarithm of the relative error via logarithm of the grid step; 3-D case, linearly varying viscosity, high viscosity contrast ($\eta_2 = \eta_3 = \eta_4 = 100$); blue line – pressure, red – v_x, black – v_y, green – v_z; line – L_1-error, dashed line – L_∞-error, line with dots – L_2-error.

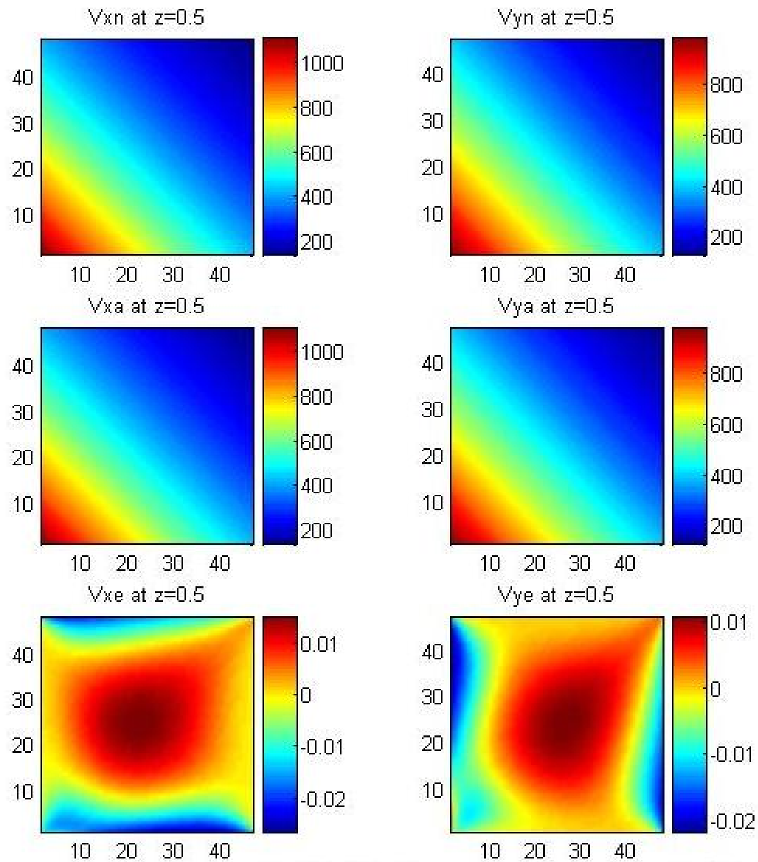

Fig. 21. Distribution of v_x and v_y; 3-D case, exponentially varying viscosity, low viscosity contrast ($\eta_2 = \eta_3 = \eta_4 = 5$).

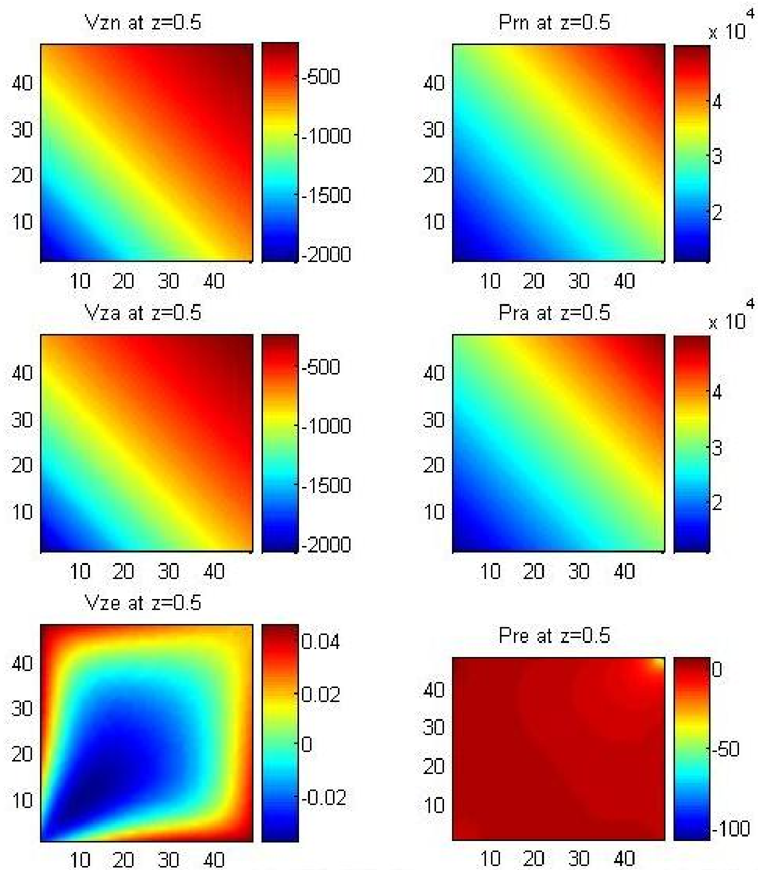

Fig. 22. Distribution of v_z and P; 3-D case, exponentially varying viscosity, low viscosity contrast ($\eta_2 = \eta_3 = \eta_4 = 5$).

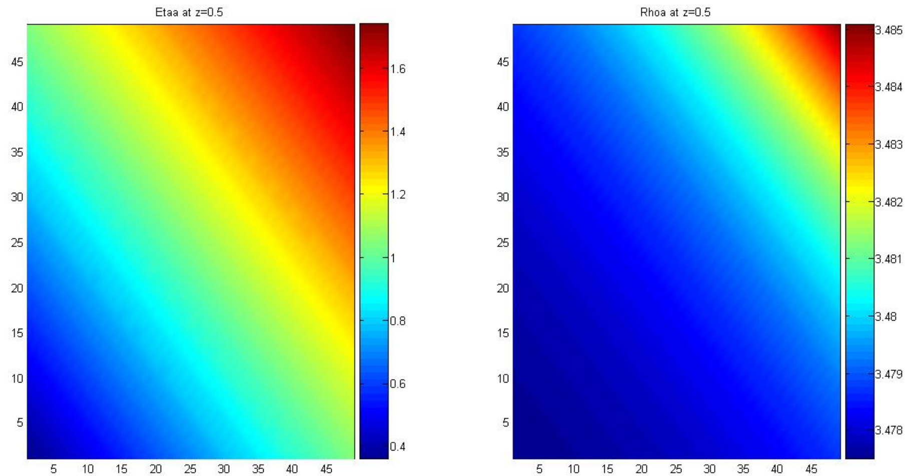

Fig. 23. Distribution of viscosity η and density ρ; 3-D case, exponentially varying viscosity, low viscosity contrast ($\eta_2 = \eta_3 = \eta_4 = 5$).

SED
5, 2203–2281, 2013

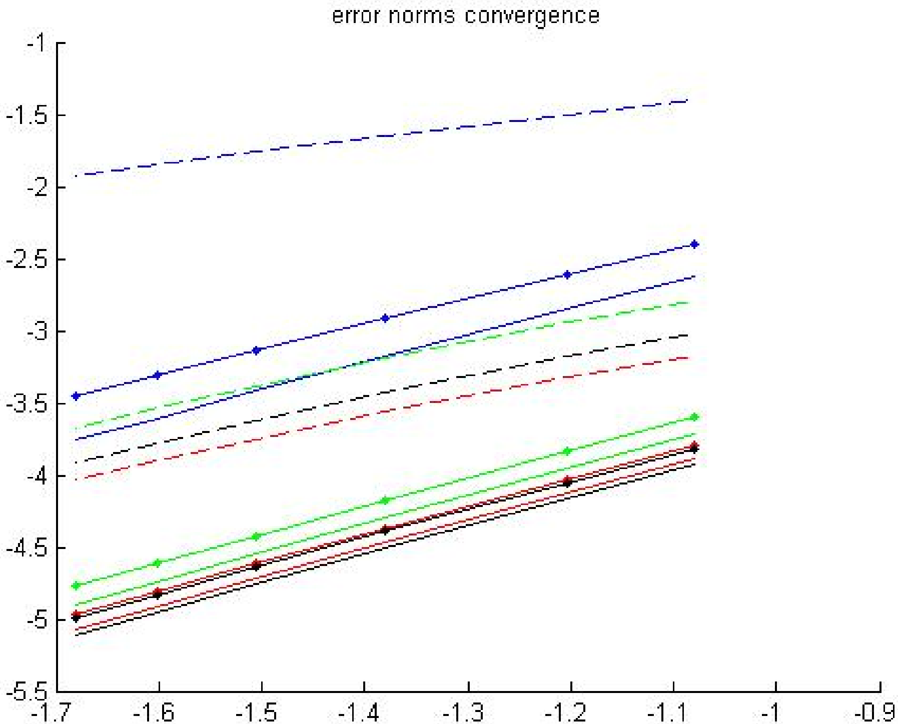

Fig. 24. Logarithm of the relative error via logarithm of the grid step; 3-D case, exponentially varying viscosity, low viscosity contrast ($\eta_2 = \eta_3 = \eta_4 = 5$); blue line – pressure, red – v_x, black – v_y, green – v_z; line – L_1-error, dashed line – L_∞-error, line with dots – L_2-error.

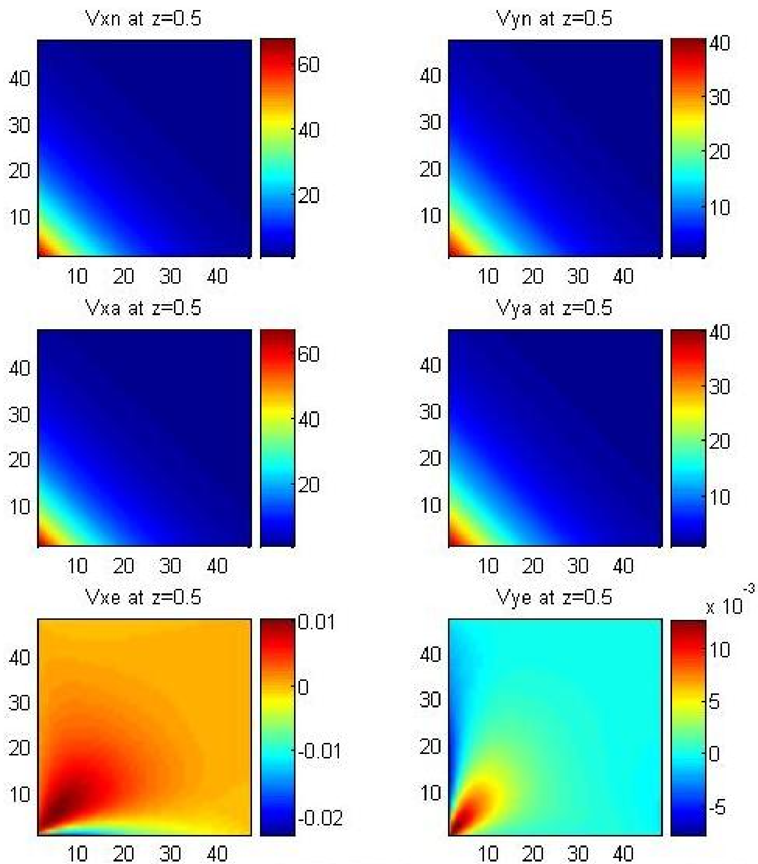

Fig. 25. Distribution of v_x and v_y; 3-D case, exponentially varying viscosity, high viscosity contrast ($\eta_2 = \eta_3 = \eta_4 = 100$).

SED
5, 2203–2281, 2013

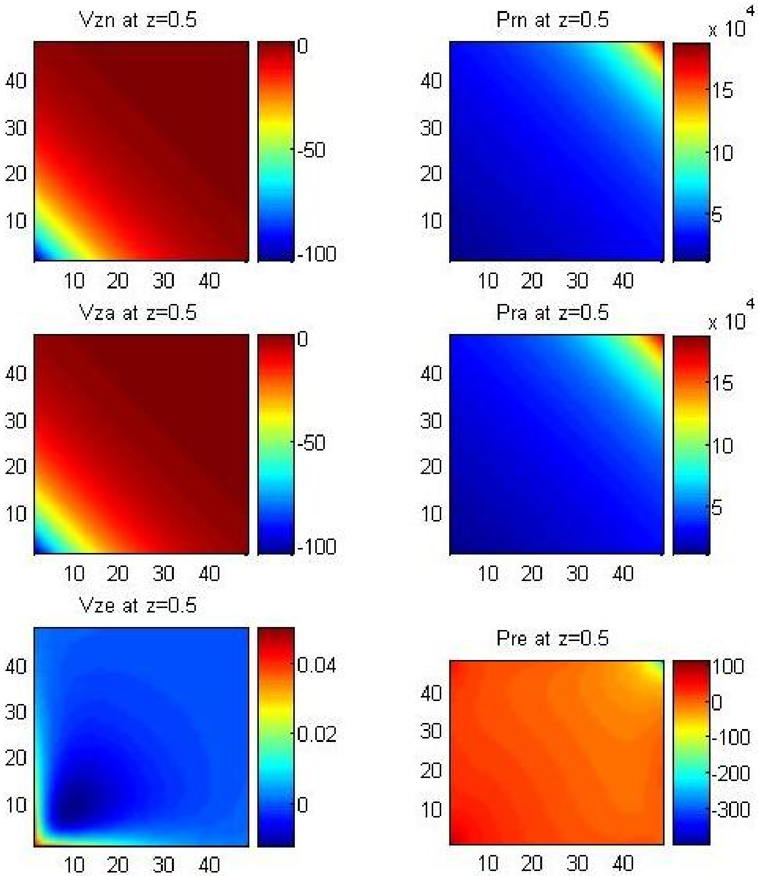

Fig. 26. Distribution of v_z and P; 3-D case, exponentially varying viscosity, high viscosity contrast ($\eta_2 = \eta_3 = \eta_4 = 100$).

SED

5, 2203–2281, 2013

Benchmarking of geodynamic Stokes problems with variable viscosity

I. Yu. Popov et al.

Title Page
Abstract | Introduction
Conclusions | References
Tables | Figures
◂◂ | ▸▸
◂ | ▸
Back | Close
Full Screen / Esc
Printer-friendly Version
Interactive Discussion

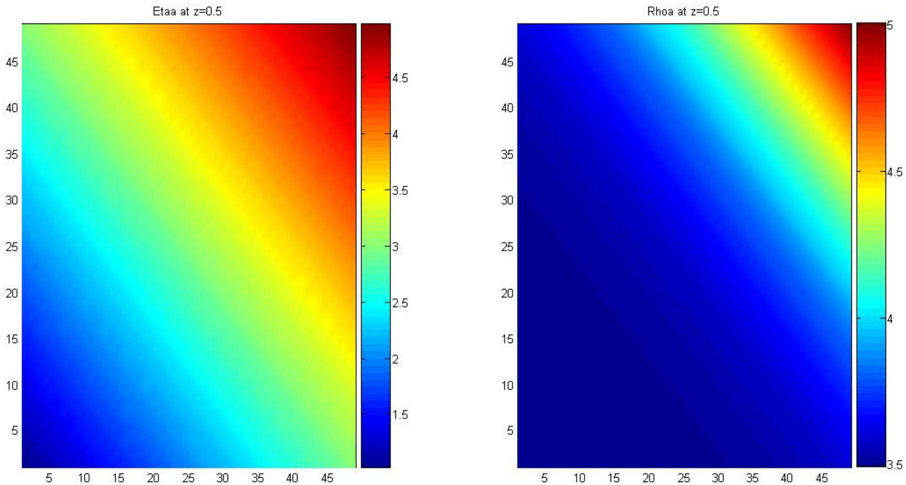

Fig. 27. Distribution of viscosity η and exponentially varying viscosity, high viscosity contrast ($\eta_2 = \eta_3 = \eta_4 = 100$).

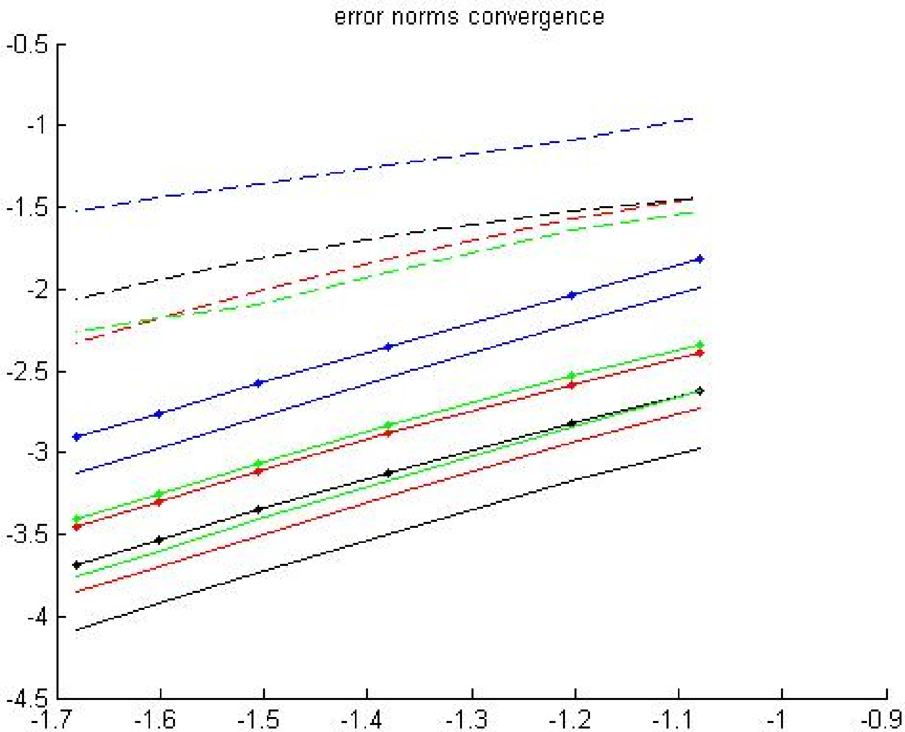

Fig. 28. Logarithm of the relative error via logarithm of the grid step; 3-D case, exponentially varying viscosity, high viscosity contrast ($\eta_2 = \eta_3 = \eta_4 = 100$); blue line – pressure, red – v_x, black – v_y, green – v_z; line – L_1-error, dashed line – L_∞-error, line with dots – L_2-error.

SED
5, 2203–2281, 2013